



MINISTRY OF AVIATION

AERONAUTICAL RESEARCH COUNCIL
REPORTS AND MEMORANDA

Use of Camber and Twist to produce Low-Drag
Delta or Swept-back Wings, without
Leading-Edge Singularities, at Supersonic Speeds

By G. M. ROPER, M.A., Ph.D.

LONDON: HER MAJESTY'S STATIONERY OFFICE

1961

PRICE £1 1 0 NET

Use of Camber and Twist to produce Low-Drag Delta or Swept-back Wings, without Leading-Edge Singularities, at Supersonic Speeds

By G. M. ROPER, M.A., Ph.D.

COMMUNICATED BY DEPUTY CONTROLLER AIR, (RESEARCH AND DEVELOPMENT)
MINISTRY OF SUPPLY

*Reports and Memoranda No. 3196**

December, 1958

Summary. Camber and twist is applied to the problem of producing low-drag wings with no leading-edge pressure singularities, at design lift. The suction peaks near the leading edges of the wing are removed and the associated adverse pressure gradients reduced. This is equivalent to keeping the pressures finite along the leading edge, and thus making the leading edge an attachment line. Linearised wing theory is used.

The optimising process of Ref. 1 is used to obtain some wings with minimum drag due to lift. Suggestions are made for modifying the load distribution and shape of the wing if required.

An outline of the general method for designing cambered and twisted wings and, in particular, those with no leading-edge load is also given.

1. *Introduction.* In Ref. 1, camber and twist is applied to the problem of reducing drag, due to incidence, of thin triangular or swept-back wings at supersonic speeds, with subsonic leading edges and supersonic or sonic trailing edges.

It is known that, unless care is taken, an infinite suction (corresponding to a singularity) will occur (according to linear theory) on an infinitely thin leading edge, giving rise to a finite thrust locally. In practice, a wing is not infinitely thin, and an infinite suction does not occur. In incompressible flow, it is well known that an equivalent thrust at the leading edge does appear, at least when there is no leading-edge separation. It is not yet known how much suction will occur in supersonic flow.

In Ref. 1, two cases were considered:

- (a) with leading edge suction forces included
- (b) with leading edge suction forces omitted

in the process of finding 'optimum' drag for given lift. In each case, the (theoretical) leading-edge suction was modified, being different from that on the uncambered wing of the same plan-form, for the same lift. This suction vanished, as it should, when the leading edges were sonic, and also became small, and tended to vanish, for 'very slender' wings (that is, when $(M^2 - 1)^{1/2} \tan \gamma \rightarrow 0$, M being the free-stream Mach number, and γ the semi-apex-angle of the wing).

* R.A.E. Report Aero. 2614, received 12th May, 1959.

In this report, wings are designed with no (theoretical) leading-edge load at design lift. By removing the suction peaks near the leading edges of the wing, the associated adverse pressure gradients are reduced, thereby (it is hoped) reducing the tendency for the boundary layer to separate. Two examples of wings of this type were given in Ref. 4, but no particular attention was then paid to obtaining a wing with low drag.

Three topics are dealt with in this report:

(i) The calculation of some further solutions of the linearised supersonic-flow equations:

In Ref. 1, the load distributions on the nine separate surfaces $z = -\delta x^{n-2s} (ky)^{2s}$ [$n(> 2s) = 1, 2, 3, 4, 5; s = 0, 1, 2$] are given, where δ is a small arbitrary constant, x is measured downstream from the apex, y is measured to starboard, and z is measured vertically upwards. In this report, solutions for $n = 6, s = 0, 1, 2$ are given; further solutions can be calculated, using the methods of Refs. 3 and 2. The load distribution on the surface $z = -\delta x |ky|$ is also given.

(ii) The design of wings with no leading-edge load:

Suitable selections of the thirteen surfaces mentioned in (i) are linearly combined to form surfaces for which the leading-edge singularities vanish. Formulae for the total lift, drag due to incidence, and positions of the centres of pressure of the surfaces are deduced, and also the interference drag terms which appear when any two surfaces are combined.

An outline of the general method for designing cambered and twisted wings, with particular reference to those with zero leading-edge load (which might be used for more extensive calculations on an electronic computer) is given in Section 6.

(iii) Application of the methods of Ref. 1 to obtain some low-drag wings with zero load on the leading edges:

Simple ('basic') surfaces with no leading-edge load are combined, and the optimising process of Ref. 1 is used to obtain some minimum-drag wings with no leading-edge load. An alternative method would be to apply the optimising process to the 'basic' surfaces mentioned in (i), with the condition that the loadings on the leading edges of the final wing are zero. The two methods are essentially the same and give the same final results. The variation of drag with lift (or incidence) of the designed wing is also calculated.

Suggestions are made for modifying the load distribution or shape of a designed wing, if this should be required.

2. The Load Distributions on the Basic Cambered and Twisted Surfaces. In Ref. 3, the linearised supersonic-flow equation is solved, and the velocity potential is obtained in terms of two kinds of Lamé functions, which are such that solutions can be applied to a swept-back plan-form with supersonic or sonic trailing edges, and the boundary conditions on the Mach cone of the apex are satisfied. The shapes of the corresponding cambered and twisted surfaces are found, it being assumed that the surfaces all lie close to the plane $z = 0$.

The load distributions corresponding to the nine basic surfaces given by equations of the form $z_r = -\delta x^{n-2s} (ky)^{2s}$ ($n > 2s$), for $n = 1$ to 5 , ($r = 1$ to 6 and 8 to 10) are given in Ref. 1, where $k = \cot \gamma$, and γ is the semi-apex-angle.

Using the methods of Ref. 3, it can be shown that the velocity potentials for the surfaces given by $n = 6$ are as follows:

TABLE 1

The velocity potentials for surfaces given by $n = 6$

$$[X \equiv (x^2 - k^2 y^2)^{1/2}]$$

Surface	Velocity potential, ϕ , on the surface
$z_{11} = -\frac{\delta}{c^5} x^6$	$\frac{V\delta F_4}{c^5 k E(\kappa)} [f_{23} x^5 + f_{24} k^2 y^2 x^3 + f_{25} k^4 y^4 x] X$
$z_{12} = -\frac{\delta}{c^5} k^2 y^2 x^4$	$\frac{V\delta F_4}{c^5 k E(\kappa)} [f_{26} x^5 + f_{27} k^2 y^2 x^3 + f_{28} k^4 y^4 x] X$
$z_{13} = -\frac{\delta}{c^5} k^4 y^4 x^2$	$\frac{V\delta F_4}{c^5 k E(\kappa)} [f_{29} x^5 + f_{30} k^2 y^2 x^3 + f_{31} k^4 y^4 x] X$

where V is the free-stream velocity, $\kappa^2 = 1 - \beta^2 \tan^2 \gamma$, $E(\kappa)$ is the complete elliptic integral of the second kind of modulus κ , and $f_{23}, f_{24}, \dots, f_{31}, F_4, F_{23}, F_{26}, F_{29}$ are functions of κ which are calculated in Appendices I to III of this report.

Formulae for the local slope, α_r , and the load per unit area, p_r , on the basic surfaces, z_r , given in Table 1, are given in Table 2 below.

Henceforth all forces are normalised by dividing by $(\pi\rho V^2 c^2)/(k^2 E(\kappa))$.

TABLE 2

The Local Slope and Loading on the Basic Surfaces z_r

r	z_r	$\alpha_r = -\frac{\partial z_r}{\partial x}$	$\left(\frac{\pi c^2}{2k}\right) p_r$
11	$-\frac{\delta}{c^5} x^6$	$\frac{6\delta}{c^5} x^5$	$\frac{\delta}{c^5} F_4 [F_{23} \frac{x^6}{X} + \{(5f_{23} - f_{24} - f_{25})x^4 + (3f_{21} - f_{25})k^2 y^2 x^2 + f_{25} k^4 y^4\} X]$
12	$-\frac{\delta}{c^5} k^2 y^2 x^4$	$\frac{4\delta}{c^5} k^2 y^2 x^3$	$\frac{\delta}{c^5} F_4 [F_{26} \frac{x^6}{X} + \{(5f_{26} - f_{27} - f_{28})x^4 + (3f_{27} - f_{28})k^2 y^2 x^2 + f_{28} k^4 y^4\} X]$
13	$-\frac{\delta}{c^5} k^4 y^4 x^2$	$\frac{2\delta}{c^5} k^4 y^4 x$	$\frac{\delta}{c^5} F_4 [F_{29} \frac{x^6}{X} + \{(5f_{29} - f_{30} - f_{31})x^4 + (3f_{30} - f_{31})k^2 y^2 x^2 + f_{31} k^4 y^4\} X]$

Formulae for calculating $f_{23}, f_{24}, \dots, f_{31}, F_4, F_{23}, F_{26}, F_{29}$ are given in Appendices I to III.

Surfaces of the form $z = -\delta x^{n-2s-1} |ky|^{2s+1}$ ($n > 2s + 1$) could also be used. The surfaces $z_2 = -\delta x^2$ and $z_{2a} = -\delta x |ky|$ are combined to form the surface z_g (See Section 3, Table 3), this being the only 'no singularity' surface, of the type considered in this report, with a non-zero pressure gradient at the apex.

For the surface $z_{2a} = -\delta x |ky|$:
the velocity potential on the surface is

$$\phi_{2a} = \frac{\delta V}{\pi k} \left[\left(\frac{1}{f_1} - 1 \right) xX + k^2 y^2 \cosh^{-1} \left| \frac{x}{ky} \right| \right] \quad ;$$

the local incidence is $\alpha_{2a} = \delta |ky|$; the (normalised) load distribution is given by:

$$\left(\frac{\pi c^2}{2k} \right) p_{2a} = \frac{\delta E(\alpha)}{\pi} \left[\frac{1}{f_1} \left(\frac{x^2}{X} + X \right) - 2X \right].$$

The formulae for f_1 is given in Appendix I; a table of values is given in Refs. 1, 2 and 3.

3. Load Distributions on Cambered and Twisted Surfaces with no Leading-Edge Load. By suitable combinations of the surfaces mentioned in Section 2, it is possible to determine the shape of a thin wing with swept-back leading edges and supersonic or sonic trailing edges, which, at design incidence, has finite pressure everywhere, the load becoming zero at the leading edges.

For all values of n , there are n surfaces of the form $z = -\delta x^{n-t} |ky|^t$ ($n > t$), where n, t , are positive integers, and $(n - 1)$ independent 'no singularity' surfaces of degree n can be formed for each value of n . If even powers only of y are used, there are $(n - 1)/2$ or $(n - 2)/2$ 'no singularity' surfaces of degree n , when n is odd or even respectively.

In this report, the thirteen surfaces for $n = 1, 2, 3, 4, 5, 6$; $t = 0, 2, 4$, and $n = 2, t = 1$ are used to determine the seven 'basic' no-singularity surfaces whose equations and local slopes are given in Tables 3 and 4 below.

Formulae for the load per unit area on these surfaces are given in Table 5, and the positions of the centres of pressure are given in Table 4.

These surfaces can then be combined to form a minimum-drag wing with no leading-edge singularities, or to satisfy other given conditions.

The same wing can be obtained from the original surfaces (given in Table 9), with the additional conditions that the leading-edge singularities vanish.

4. Formulae for the Calculation of Minimum Drag for Given Wing Combinations. Formulae for the local surface slope, position of centre of pressure, load per unit area, lift and drag for a surface of the form $z = \sum (A_r z_r)$, where A_r are constants, are given in Ref. 1. The formulae are given, in a slightly different form below.

Writing $(A_r L_r)/L = a_r$, where L_r is the (normalised) lift of surface z_r , and L the total (normalised) lift, the equation of the final surface can be written in the form:

$$z = \frac{kE(\alpha)}{2\pi} C_{L0} \sum \left(\frac{a_r}{L_r} z_r \right) + F(y) \text{ for a triangular wing,} \quad (1)$$

TABLE 3

Formulae for the Shape, z_r , and Local Surface Slopes, α_r , of the 'Basic' Cambered and Twisted Surfaces, with No Leading-Edge Load

(Formulae for $f_4, f_5 \dots F_{17}, \dots$ are given in Appendix I)

r	z_r	α_r
a	$-\delta (f_4 x^3 - f_5 k^2 y^2 x)$	$\delta (3f_4 x^2 - f_5 k^2 y^2)$
b	$-\delta (f_{10} x^4 - 2f_{11} k^2 y^2 x^2)$	$4\delta (f_{10} x^3 - f_{11} k^2 y^2 x)$
c	$+\delta (F_{17} x^5 + F_{14} k^2 y^2 x^3)$	$-\delta (5F_{17} x^4 + 3F_{14} k^2 y^2 x^2)$
d	$-\delta (F_{20} k^2 y^2 x^3 + F_{17} k^4 y^4 x)$	$\delta (3F_{20} k^2 y^2 x^2 + F_{17} k^4 y^4)$
e	$-\delta (F_{26} x^6 - F_{23} k^2 y^2 x^4)$	$\delta (6F_{26} x^5 - 4F_{23} k^2 y^2 x^3)$
f	$-\delta (F_{29} k^2 y^2 x^4 - F_{26} k^4 y^4 x^2)$	$\delta (4F_{29} k^2 y^2 x^3 - 2F_{26} k^4 y^4 x)$
g	$-\delta (x^2 - \frac{\pi}{E(x)} x ky)$	$\delta (2x - \frac{\pi}{E(x)} ky)$

TABLE 4

Positions of the Centres of Pressure of Cambered and Twisted Triangular Surfaces

v_r = distance downstream of the apex, in root-chord lengths
(The equations of the surfaces $r = 1$ to 13 are given in Table 9, at the end of this report)

r	v_r	r	v_r
1	2/3		
2 or 2a	3/4	g	3/4
3 or 5	4/5	a	4/5
4 or 6	5/6	b	5/6
8, 9, or 10	6/7	c or d	6/7
11, 12, or 13	7/8	e or f	7/8

TABLE 5

Formulae for the (Normalised) Load per unit area, p_r , on the Basic
'No Singularity' Surfaces

r	$\left(\frac{\pi c^2}{2k}\right) p_r$
a	$3\delta x X$
b	$4\delta(4x^2 - k^2 y^2) X$
c	$\delta F_3[\{F_{14}(4f_{17} - f_{18} - f_{19}) - F_{17}(4f_{14} - f_{15} - f_{16})\}x^3$ $+ \{F_{14}(2f_{18} - f_{19}) - F_{17}(2f_{15} - f_{16})\}k^2 y^2 x] X$
d	$\delta F_3[\{F_{17}(4f_{20} - f_{21} - f_{22}) - F_{20}(4f_{17} - f_{18} - f_{19})\}x^3$ $+ \{F_{17}(2f_{21} - f_{22}) - F_{20}(2f_{18} - f_{19})\}k^2 y^2 x] X$
e	$\delta F_4[\{F_{26}(5f_{23} - f_{24} - f_{25}) - F_{23}(5f_{26} - f_{27} - f_{28})\}x^4$ $+ \{F_{26}(3f_{24} - f_{25}) - F_{23}(3f_{27} - f_{28})\}k^2 y^2 x^2$ $+ \{F_{26}f_{25} - F_{23}f_{28}\}k^4 y^4] X$
f	$\delta F_4[\{F_{29}(5f_{26} - f_{27} - f_{28}) - F_{26}(5f_{29} - f_{30} - f_{31})\}x^4$ $+ \{F_{29}(3f_{27} - f_{28}) - F_{26}(3f_{30} - f_{31})\}k^2 y^2 x^2$ $+ \{F_{29}f_{28} - F_{26}f_{31}\}k^4 y^4] X$
g	$2\delta X$

$$z = \frac{kE(\kappa)}{2\pi(1-a)} C_{L0} \sum \left(\frac{a_r}{L_r} z_r \right) + F(y) \text{ for a swept-back wing} \quad (2)$$

with supersonic or sonic trailing edges, where C_{L0} is the design lift coefficient, based on the area of the plan-form, $F(y)$ is a small arbitrary function of y , and a is the ratio $\tan \gamma / \tan \sigma$, γ , σ being the leading-edge and trailing-edge semi-apex-angles respectively.

The corresponding loading coefficients are:

$$C_P = \frac{2}{\pi} C_{L0} \sum \left(\frac{a_r}{L_r} \frac{\pi c^2}{2k} p_r \right) \text{ for a triangular wing,} \quad (3)$$

$$C_P = \frac{2}{\pi(1-a)} C_{L0} \sum \left(\frac{a_r}{L_r} \frac{\pi c^2}{2k} p_r \right) \text{ for a swept-back wing.} \quad (4)$$

For each wing, the (normalised) drag/(lift)² is given by:

$$d = \sum \left(a_r^2 d_r + a_r a_s d_{r,s} \right) \quad (r < s); \quad (5)$$

$$\frac{C_D}{C_L^2} = \frac{kE(\chi)}{2\pi} d \text{ for a triangular wing,} \quad (6)$$

$$\frac{C_D}{C_L^2} = \frac{kE(\chi)}{2\pi(1-a)} d \text{ for a swept-back wing,} \quad (7)$$

where C_L, C_D are the lift and drag coefficients.

The distance of the centre of pressure downstream of the apex, in root chord lengths, is

$$v = \sum (a_r v_r), \quad (8)$$

where v_r is the value of v for surface z_r .

Formulae for z_r, p_r for the separate triangular or swept-back 'no singularity' surfaces are given in Tables 3 and 5. Formulae for $v_r, d_r, d_{r,s}$ for triangular 'no singularity' surfaces are given in Tables 4, 12 and 14; the formulae for swept-back surfaces can be deduced from results given in Ref. 1. Some further results for swept-back wings and modified methods for some of the calculations will be published later.

The minimum values of d ($\equiv d_{\text{opt}}$) and the appropriate coefficients, a_r , are functions of the $d_r, d_{r,s}$ of the surfaces combined¹. All forces were normalised by dividing by $\pi\rho V^2 c^2 / (k^2 E(\chi))$, but the ratio d/d_1 , where d_1 is the value of d for the corresponding flat wing, is independent of the normalising factor.

For the combination of n surfaces, $r = a, b, \dots, n$,

$$\frac{a_r}{\Delta_r} = \frac{2d_{\text{opt}}}{\Delta_N} = \frac{1}{\sum_{r=a}^n \Delta_r}, \quad (9)$$

where

$$\Delta_N \equiv \begin{vmatrix} 2d_a & d_{a,b} & d_{a,c} \dots d_{a,n} \\ d_{b,a} & 2d_b & d_{b,c} \dots d_{b,n} \\ \vdots & \vdots & \vdots \\ d_{n,a} & d_{n,b} & d_{n,c} \quad 2d_n \end{vmatrix}, \quad (10)$$

and Δ_r ($r = a, b, \dots, n$) is equal to Δ_N , with each term in the r th column (or row) replaced by 1.

$$\text{Also} \quad d_{\text{opt}} = \sum_{r=a}^n \left(a_r^2 d_r + a_r a_s d_{r,s} \right), \quad r < s, \quad (11)$$

where a_r, a_s are given by (9).

Alternative formulae giving the values of a_r and d_{opt} , which are more suitable when an electronic computer is used, are:

$$d_{\text{opt}} = 1 \left/ \left[2 \sum_{r=a}^n X_r \right] \right., \quad (12)$$

$$a_r = 2X_r d_{\text{opt}}, \quad (13)$$

where X_r are the roots of the linear equations

$$\sum_{r=a}^n (d_{s,r} X_r) = 1, \quad (14)$$

$s = a, b, \dots, n$, and $d_{r,r} \equiv 2d_r$.

Another formula giving d_{opt} , (useful for checking), is

$$d_{\text{opt}} = 1 / \left[4 \sum_{r=a}^n (X_r^2 d_r + X_r X_s d_{r,s}) \right] \dots r < s \quad (15)$$

Another check on calculations is:

$$\sum_{r=a}^n a_r = 1. \quad (16)$$

Formulae for the calculation of minimum drag for given wing combinations, when the centre of pressure is fixed at design C_L , are given in Ref. 1.

5. Modifications to Designed Wings.

(a) Position of Centre of Pressure.

If the position of the centre of pressure of a designed 'no singularity' (or any other) wing is unfavourable, the position can be altered by superimposing a suitable combination of other solutions, and the corresponding changes in drag/(lift)² can be calculated (Positions of the centres of pressure of the separate surfaces are given in Table 4).

Formulae for the calculation of minimum drag, when the centre of pressure is fixed at design C_L , are given in Ref. 1.

(b) Non-zero Pressure Gradient at the Apex.

For the wings discussed in this report, the loading at the apex is zero. The chordwise pressure gradient at the apex for all the basic 'no singularity' surfaces, except surface z_g , is also zero. Therefore, if a pressure gradient at the apex is desired, surface z_g must be included in the combination taken. But it is found, in general, that the drag/(lift)² increases fairly quickly with the increase of a favourable pressure gradient at the apex.

(c) Modification of Adverse Pressure Gradient.

When a 'no singularity' wing is designed for minimum drag/(lift)², it is, in some cases, found that there is a (theoretical) adverse pressure gradient along the root chord, towards the trailing edge. This can be partly remedied by superposing solutions with more favourable load distributions; in particular, the superposition of solutions having zero load at the trailing edge of the root chord has, in general, the effect of 'flattening' the root chord load 'pattern'. Or, it is possible first to form solutions which give zero load at the trailing edge of the root chord, and then to find a minimum-drag wing by combining these solutions. Using the seven basic surfaces given in Table 3, there are six independent

'no singularity' surfaces having zero load on the root chord at the trailing edge, viz,:

$$\begin{aligned} z_A &= bz_a - az_b, & z_B &= cz_a - az_c, \\ z_C &= dz_a - az_d, & z_D &= ez_a - az_e, \\ z_E &= fz_a - az_f, & z_N &= az_g - gz_a, \end{aligned}$$

where a, b, c, d, e, f, g are the coefficients of $x^2, x^3, x^4, x^4, x^5, x^5, x$ respectively in the formulae for $(\pi c^2/2k)p_r$ ($r = a, \dots, g$) when $y = 0$ (See Table 5).

(d) *Modification of Shape of Camber Surface.*

(i) The equation of a camber surface has been found in the form $z = \sum (A_r z_r) + F(y)$, where $F(y)$ is an arbitrary function of y , which does not affect the load distribution, or the downwash. $F(y)$ can be chosen to satisfy any suitable condition: e.g., $z = 0$ at the leading edge or trailing edge, or at any other chordwise position.

(ii) The chordwise local slope (and also the spanwise local slope if, for example, $F(y)$ satisfies one of the conditions suggested above) can be modified by taking $z = \sum (A_r z_r) + F_1(y) + \alpha x$ as the equation of the camber surface, and placing the wing at the original design incidence plus incidence α . With the linear-theory approximations, the theoretical load distribution, lift, drag, and position of the centre of pressure of the modified wing are the same as for the original wing.

The modifications suggested above are obviously only a few of those which could be made. Many more are possible, using the basic solutions given in this report, or higher-order solutions constructed from the general solutions given in Ref. 3 (See also Section 6 of this report).

6. *General Formulae for the Design of Delta Wings, or Swept-back Wings.* Using the general results given in Ref. 3, it can be shown that, for all positive integral values of n , there are solutions of the linearised supersonic flow equation for the velocity potential, ϕ , (on the wing), of the form:

$$\phi_n^m = \frac{\delta V}{c^{n-1} k E(\kappa)} \prod_{r=1}^{(n-1)/2} \left[\kappa^2 x^2 - \frac{c_r}{1-c_r} (1-\kappa^2) X^2 \right]_m X, \quad (m = 1, 2, \dots, (n+1)/2; c_r \geq 0), \quad \text{if } n \text{ is odd}; \quad (17a)$$

$$\phi_n^m = \frac{\delta V}{c^{n-1} k E(\kappa)} \kappa x \prod_{r=1}^{(n-2)/2} \left[\kappa^2 x^2 - \frac{d_r}{1-d_r} (1-\kappa^2) X^2 \right]_m X, \quad (m = 1, 2, \dots, n/2; d_r \geq 0), \quad \text{if } n \text{ is even}, \quad (17b)$$

where (Ref. 3, Appendix III) $X = (x^2 - k^2 y^2)^{1/2}$, the values of c_r ($r = 1, 2, \dots, (n-1)/2$), for each value of m , are given by the $(n-1)/2$ equations

$$\frac{1}{2c_r} \left\{ 5 + \frac{\kappa^2}{c_r - \kappa^2} + \frac{3}{c_r - 1} \right\} + 2 \sum_{s=1}^{(n-1)/2} \left(\frac{1}{c_r - c_s} \right) = 0, \quad s \neq r, \quad (18a)$$

and the values of d_r ($r = 1, 2, \dots, (n-2)/2$), for each value of m , are given by the $(n-2)/2$ equations

Alternative equations for calculating a_s, b_s, c_r, c_s are given in Appendix 6.

The corresponding loading coefficients are given by

$$C_P = \frac{4}{V} \frac{\partial \phi_n^m}{\partial x}. \quad (24)$$

Hence, on the wing:

$$\begin{aligned} (C_P)_n = & \frac{4\delta}{c^{n-1}kE(\kappa)} \prod_{r=a}^{(n-1)/2} \left[\left\{ \kappa^2 x^2 - \frac{c_r}{1-c_r} (1-\kappa^2)X^2 \right\} \left\{ \frac{x}{X} + \right. \right. \\ & \left. \left. + 2xX \sum_{r=1}^{(n-1)/2} \left(\frac{\kappa^2 - c_r}{(\kappa^2 - c_r)x^2 + c_r(1-\kappa^2)k^2y^2} \right) \right\} \right], \text{ if } n \text{ is odd;} \end{aligned} \quad (25a)$$

and

$$\begin{aligned} (C_P)_n = & \frac{4\delta\kappa}{c^{n-1}kE(\kappa)} \prod_{r=1}^{(n-2)/2} \left[\left\{ \kappa^2 x^2 - \frac{d_r}{1-d_r} (1-\kappa^2)X^2 \right\} \left\{ \frac{x^2}{X} + X + \right. \right. \\ & \left. \left. + 2x^2X \sum_{r=1}^{(n-2)/2} \left(\frac{\kappa^2 - d_r}{(\kappa^2 - d_r)x^2 + d_r(1-\kappa^2)k^2y^2} \right) \right\} \right], \text{ if } n \text{ is even.} \end{aligned} \quad (25b)$$

The surfaces given by equations (22a) and (22b) can now be combined to form wings with no leading-edge singularities.

For each value of n , $(n-1)/2$ (if n is odd), or $(n-2)/2$ (if n is even), independent cambered surfaces with zero leading-edge load can be found by combining surfaces of the form given above. These surfaces could be taken as:

$$\begin{aligned} z_{r,s} \equiv (z_r - z_s)_n, \quad r,s = 1,2,\dots,(n+1)/2 \text{ if } n \text{ is odd,} \\ = 1,2,\dots,n/2 \text{ if } n \text{ is even, } r < s. \end{aligned} \quad (26)$$

A general equation of 'no singularity' surfaces (containing even powers of y only) is

$$z = \sum_{n=0}^{\infty} \sum_{r,s=1}^{(n-1)/2 \text{ or } (n-2)/2} (A_{r,s} z_{r,s}), \quad (r < s), \quad (27)$$

where $A_{r,s}$ are arbitrary constants, which can be chosen to satisfy given conditions.

The corresponding loading coefficient is

$$C_P = \sum_n \sum_{r,s} [A_{r,s} (C_P)_{r,s}] = \sum_n \sum_{r,s} [A_{r,s} \{ (C_P)_r - (C_P)_s \}_n]. \quad (28)$$

There are also $(n-1)/2$ (if n odd), or $n/2$ (if n even), surfaces of the form $z_r = -\delta x^{n-r} |ky|^r$, and their corresponding loading coefficients (Surface $z = -\delta x |ky|$ has been used in one of the examples given in this report).

If these surfaces are combined with each other, and with those given above, to form surfaces $z_{r,s}$, so that leading-edge singularities are eliminated, it can be shown that the general equation (in the form

of a polynomial) of 'no singularity' surfaces can be written

$$z = \sum_{n=0}^{\infty} \sum_{r,s=1}^{n-1} (B_{r,s} z_{r,s}), \quad (y < s). \quad (29)$$

The lift and drag coefficients are given by

$$C_L = \left(\int C_p dS \right) / S, \quad (30)$$

$$C_D = \left(\int -C_p \frac{\partial z}{\partial x} dS \right) / S; \quad (31)$$

the pitching moment coefficient about the leading edge apex is

$$C_M = \left(\int x C_p dS \right) / (cS); \quad (32)$$

and the distance, in root chord lengths, of the centre of pressure from the leading edge apex is

$$v = C_M / C_L. \quad (33)$$

The integration is over the wing plan-form, of which the area is S , and the root chord c .

Formulae for evaluating certain double integrals, which are required for the calculation of the lift and drag of triangular and swept-back wings, are given in Appendices V and VI of Ref. 1. Some further formulae are given in Appendix IV of this report.

7. *Variation of Drag with Lift.* If a designed 'no singularity' wing is placed in the free stream at other than design incidence, there is a (theoretical) leading-edge suction force. If C_L is the lift coefficient in the new position, the variation of the drag coefficient, C_D , with C_L is given by: (for a triangular wing)

$$C_D = \frac{kE(\gamma)}{2\pi} \left[t_1 C_L^2 + (d_{1,0} - 2t_1) C_L C_{L0} + (t_1 + d_0 - d_{1,0}) C_{L0}^2 \right], \quad (34)$$

where C_{L0} is the design lift coefficient, d_0 is the design value of d , t_1 is the (normalised) drag/(lift)² of the flat wing, with suction included, and

$$d_{1,0} = \sum (a_r d_{1,r}). \quad (35)$$

The variation of the pressure drag coefficient, C_{DP} , (suction ignored) is given by

$$C_{DP} = \frac{kE(\gamma)}{2\pi} \left[d_1 C_L^2 + (d_{1,0} - 2d_1) C_L C_{L0} + (d_1 + d_0 - d_{1,0}) C_{L0}^2 \right], \quad (36)$$

d_1 being the value of (normalised) drag/(lift)² for the flat wing, with suction ignored.

The formulae for the flat triangular wing are:

$$C_D = \frac{kE(\kappa)}{2\pi} t_1 C_L^2, \quad (37)$$

$$C_{D_P} = \frac{kE(\kappa)}{2\pi} d_1 C_L^2. \quad (38)$$

$d_{1,0}$ is the 'interference' term for the flat wing and the designed 'no singularity' wing.

The separate 'interference' terms, $d_{1,r}$, for the triangular surfaces used in this report are:

$$\begin{aligned} d_{1,a} &= \frac{1}{\bar{L}_a} (f_4 L_3 d_{1,3} - f_5 L_5 d_{1,5}); \\ d_{1,b} &= \frac{1}{\bar{L}_b} (f_{10} L_4 d_{1,4} - 2f_{11} L_6 d_{1,6}); \\ d_{1,c} &= -\frac{1}{\bar{L}_c} (F_{17} L_8 d_{1,8} + F_{14} L_9 d_{1,9}); \\ d_{1,d} &= \frac{1}{\bar{L}_d} (F_{20} L_9 d_{1,9} + F_{17} L_{10} d_{1,10}); \\ d_{1,e} &= \frac{1}{\bar{L}_e} (F_{26} L_{11} d_{1,11} - F_{23} L_{12} d_{1,12}); \\ d_{1,f} &= \frac{1}{\bar{L}_f} (F_{29} L_{12} d_{1,12} - F_{26} L_{13} d_{1,13}); \\ d_{1,g} &= \frac{1}{4} - \frac{1}{E(\kappa)}. \end{aligned} \quad (39)$$

Some graphs showing the variation of C_D and C_{D_P} with C_L are shown in Figs. 8 and 13.

The formulae giving the variation of C_D , C_{D_P} with C_L , for a swept-back wing, are of the same form as (32) to (36), with denominator $2\pi(1 - a)$ instead of 2π , and the appropriate values of d_0 , $d_{1,r}$, d_1 , t_1 .

8. Numerical Examples. A number of examples of delta wings, cambered and twisted so that there are no leading-edge loads, have been investigated. The theoretical shape of camber surface, and load distribution of three delta wings with finite leading edge pressures, and also the variation of drag with lift, are shown in Figs. 1 to 13. Some details concerning these wings are given below: (x , y , z are measured in root chord lengths; $z = 0$ at the trailing edge.)

Wing 1

Wing 1 was designed for minimum drag for given lift.

$$\begin{aligned} \beta \tan \gamma &= 0.614, & \kappa^2 &= 0.6231, & M &= 2.5; \\ \gamma &= 15 \text{ deg}, & k &= 2 + \sqrt{3}, & \text{aspect ratio} &= 1.0718. \end{aligned}$$

The shape of the camber surface is given by:

$$z/C_{L0} = G(A_a z_a + A_b z_b + A_c z_c + A_d z_d), \quad (\text{Fig. 1})$$

where

$$G = kE(x)/(2\pi) = 0.763720,$$

$$A_a = 23.197489, \quad A_b = -10.785131,$$

$$A_c = 5.406638, \quad A_d = 1.211762;$$

$$z_a = 0.6622(1 - x^3) - 2.5134k^2y^2(1 - x),$$

$$z_b = 2.3670(1 - x^4) - 5.6642k^2y^2(1 - x^2),$$

$$z_c = 2.1590(1 - x^5) - 4.1494k^2y^2(1 - x^3),$$

$$z_d = 0.6533k^2y^2(1 + x^3) - 2.1590k^4y^4(1 - x).$$

The loading coefficient at design incidence is given by:

$$C_P/C_{L0} = (2/\pi)(A_a P_a + A_b P_b + A_c P_c + A_d P_d), \quad (\text{Figs. 2 and 3})$$

where

$$P_a = 3x(x^2 - k^2y^2)^{1/2},$$

$$P_b = 4(4x^2 - k^2y^2)(x^2 - k^2y^2)^{1/2},$$

$$P_c = (19.482989x^3 - 7.609962xk^2y^2)(x^2 - k^2y^2)^{1/2},$$

$$P_d = (0.172987x^3 + 1.593199xk^2y^2)(x^2 - k^2y^2)^{1/2},$$

$$d/d_1 = 0.8966 \quad (\Delta d/d_1) \text{ per cent} = 10.34 \text{ per cent},$$

$$t_1/d_1 = 0.6930,$$

$$(t_1)_{s/2}/d_1 = 0.8465, \quad ((\Delta d)_{s/2}/d_1) \text{ per cent} = -5.01 \text{ per cent}.$$

where $d = \text{drag}/(\text{lift})^2$,

$d_1 = \text{drag}/(\text{lift})^2$ for flat wing, suction omitted,

$t_1 = \text{drag}/(\text{lift})^2$ for flat wing, full suction included,

$(t_1)_{s/2} = \text{drag}/(\text{lift})^2$ for flat wing, half-suction included,

$$\Delta d = d_1 - d, \quad (\Delta d)_{s/2} = (t_1)_{s/2} - d.$$

Wing 2

Wing 1 was modified so that $C_P = 0$ at the trailing edge of the root chord, and the chordwise adverse pressure gradient along the root chord reduced.

$$\beta \tan \gamma \simeq 0.614, \quad \alpha^2 = 0.6231, \quad M = 2.5;$$

$$\gamma = 15 \text{ deg}, \quad k = 2 + \sqrt{3}, \quad \text{aspect ratio} = 1.0718.$$

Design lift coefficient = 0.1.

The equation of the camber surface is:

$$z = 0.556(1-x)[0.1759(1+x+x^2) - 1.0584x^3 + 0.6770x^4 - 0.0033x^5 - \\ - k^2y^2(1.6947 - 2.9901x + 1.1627x^2 - 0.0055x^3) - \\ - 0.4603k^4y^4] \quad (\text{Figs. 4 and 5}).$$

The loading coefficient at design incidence is:

$$C_p = [x(2.5919 - 5.4372x + 2.8626x^2 - 0.0173x^3) + \\ + k^2y^2(1.3593 - 0.9540x + 0.0082x^2) + \\ + 0.0001k^4y^4](x^2 - k^2y^2)^{1/2}. \quad (\text{Figs. 6 and 7})$$

Distance of the centre of pressure from the apex = 0.6562 root chord lengths.

$$d/d_1 = 0.8409, \quad (\Delta d/d_1) \text{ per cent} = 15.91 \text{ per cent}, \\ t_1/d_1 = 0.6930, \\ (t_1)_{s/2}/d_1 = 0.8465, \quad ((\Delta d)_{s/2}/d_1) \text{ per cent} = 0.56 \text{ per cent}.$$

Wing 3

Wing 3 was designed for minimum drag for given lift.

$$\beta \tan \gamma = 0.3, \quad \kappa^2 = 0.91, \quad M \approx 1.56205; \\ \gamma \approx 14^\circ 2', \quad k = 4 \quad \text{aspect ratio} = 1.$$

The shape of the camber surface is given by:

$$z/C_{L_0} = (1-x)[0.925579(1+x+x^2) - 5.540635x^3 + \\ + 3.423581x^4 - k^2y^2(10.911018 - 20.823776x + 6.854739x^2) - \\ - 5.539211k^4y^4]. \quad (\text{Figs. 9 and 10}).$$

The loading coefficient at design incidence is given by:

$$C_p/C_{L_0} = [x(31.088880 - 69.630130x + 32.513480x^2) \\ + k^2y^2(17.407533 - 12.009394x)](x^2 - k^2y^2)^{1/2}.$$

Distance of the centre of pressure from the apex = 0.6478 root chord lengths.

$$d/d_1 = 0.6339, \quad (\Delta d/d_1) \text{ per cent} = 36.6 \text{ per cent}, \\ t_1/d_1 = 0.5650, \\ (t_1)_{s/2}/d_1 = 0.7825, \quad ((\Delta d)_{s/2}/(t_1)_{s/2}) \text{ per cent} = 19.0 \text{ per cent}.$$

Models of these three wings are being made, and will be tested in the 8-ft Tunnel at the Royal Aircraft Establishment, Bedford.

From a considerable number of examples investigated, it seems that the minimum drag for given lift of a delta wing, cambered and twisted so that the leading-edge loading is zero, is slightly greater than the drag of the uncambered wing (with full suction) for the lower values of $\beta \tan \gamma$, but less than the drag of the uncambered wing for larger values of $\beta \tan \gamma$. For $\beta \tan \gamma = 1$ (that is, sonic leading edges), a percentage drag reduction of about 10 per cent is predicted. If only half-suction forces are included for the uncambered wing, there is a possible (theoretical) percentage drag reduction (with infinite pressures on leading edges eliminated), increasing from about 10 per cent (for $\beta \tan \gamma = 1$) to $33\frac{1}{2}$ per cent (for $\beta \tan \gamma \rightarrow 0$, that is, for very slender wings). It is assumed here that separation reduces the suction on the flat wing by one half, whereas no separation takes place on the cambered wing, which, perhaps, makes the comparison not quite fair.

9. *Conclusion.* Camber and twist has been applied to the problem of producing low-drag delta or swept-back wings, with subsonic leading edges, but with the (theoretical) infinite leading-edge pressures eliminated. Some delta wings have been designed and suggestions made for modifying the load distribution and shape of the wings if required.

For the lower values of $\beta \tan \gamma$, most of the predicted drag reduction on the uncambered wing due to leading-edge suction can (theoretically) also be obtained by camber and twist. For values of $\beta \tan \gamma$ near to one, a drag reduction higher than that due to suction is predicted.

An outline of the general method for designing cambered and twisted wings, with special reference to wings with infinite leading-edge pressures eliminated, is given in Section 6.

It is hoped that some results for cropped delta wings and fully tapered and cropped swept-back wings will be published in a further report.

Acknowledgements. Acknowledgements are due to Miss J. Parker and Miss R. Hensby for their help with the computations, to Miss R. Hensby for the careful preparation of the drawings, and to Miss A. Paton for calculating the results of Appendix II on DEUCE.

LIST OF SYMBOLS

A	Coefficient depending on \varkappa (<i>See</i> Appendix II)
A_1, A_2, A_3	Coefficients depending on \varkappa (<i>See</i> Appendix III)
A_r	Constant coefficients (<i>See</i> Section IV)
a_m	A Lamé coefficient (<i>See</i> Appendix II)
$a_r = A_r L_r / L$	
$a = h/k$	
B	Coefficient depending on \varkappa (<i>See</i> Appendix II)
B_1, B_2, B_3	Coefficients depending on \varkappa (<i>See</i> Appendix III)
b_m	A Lamé coefficient (<i>See</i> Appendix III)
C_1, C_2, C_3	Coefficients depending on \varkappa (<i>See</i> Appendix III)
C_D	Drag coefficient
C_{DP}	Pressure drag coefficient
C_L	Lift coefficient
C_{L0}	Design lift coefficient
C_M	Pitching-moment coefficient
C_P	Loading coefficient ($= -2 \times$ pressure coefficient)
c	Length of root chord
c_r	Zeros of Lamé functions (Appendix III and Section 6)
D	(Normalised) drag
D_r	(Normalised) drag of surface, z_r
$D_{r,s} = D_{s,r}$	(Normalised) 'interference drag' of surfaces z_r, z_s
$d = D/L^2$	
d_r	Zeros of Lamé functions (in Appendix III and Section 6 only)
$d_r = D_r/L_r^2$	
d_1	(Normalised) drag/(lift) ² for flat wing (suction ignored)

LIST OF SYMBOLS—*continued*

$d_{r,s}$	=	$D_{r,s}/(L_r L_s)$
$E(\kappa)$		Complete elliptic integral of the second kind of modulus κ
$f_1, f_4, \dots, f_{31};$ $F_1, F_2, F_3, F_4;$ F_{14}, \dots, F_{29}	}	Functions of κ given in Appendix I
h	=	$\cot \sigma$
$I_{2m,n}$ $I_{2m+1,n}$	}	See Appendix IV
\tilde{J}_m	=	$\frac{1 - \kappa^2}{E(\kappa)} P_n^m(1) \int_1^\infty \frac{d}{dt} \left[\frac{1}{t [P_n^m(t)]^2 (t^2 - \kappa^2)^{1/2}} \right] \frac{dt}{(t^2 - 1)^{1/2}}$
$K(\kappa)$		Complete elliptic integral of the first kind of modulus κ
k	=	$\cot \gamma$
L		(Normalised) lift
L_r		(Normalised) lift of surface z_r
$L_{2m,n}$ $L_{2m+1,n}$	}	See Appendix IV
M	=	Mach number
$P_n^m(t)$	=	$\prod_{n=1}^{(n-1)/2} (t^2 - c_r)$ if n is odd $t \prod_{n=1}^{(n-2)/2} (t^2 - d_r)$ if n is even
p_r		(Normalised) load per unit area of surface z_r
S		Area of wing plan-form
t_1		(Normalised) drag/(lift) ² for flat wing, suction included
V		Free-stream velocity
X	=	$(x^2 - k^2 y^2)^{1/2}$
X_r	=	$a_r / (2d_{opt})$ (<i>cf.</i> equations (13) and (14))

LIST OF SYMBOLS—*continued*

x	Chordwise co-ordinate (measured downstream from the apex)
y	Spanwise co-ordinate (positive to starboard)
z	Normal co-ordinate (positive upwards)
α	Local slope ($= -\partial z/\partial x$)
α_r	Local slope of surface z_r
$\beta =$	$(M^2 - 1)^{1/2}$
γ	Apex semi-angle
Δ	<i>See</i> Appendix III
Δ_r	<i>cf.</i> equation (9)
Δ_N	<i>cf.</i> equations (9) and (10)
$\Delta d =$	$d_1 - d$
δ	Small dimensionless constant
$\kappa =$	$(1 - \beta^2 \tan^2 \gamma)^{1/2}$
λ_m	Coefficients depending on κ (<i>See</i> Appendix III)
μ	Argument of Lamé function (<i>See</i> Tables 7 and 8)
ν	Distance of centre of pressure, in root chord lengths, from the apex
ν_r	Value of ν for surface z_r
ρ	Free-stream density
σ	Apex semi-angle of trailing edge (of a swept-back wing)
ϕ	Velocity potential

REFERENCES

<i>No.</i>	<i>Author</i>	<i>Title, etc.</i>
1	G. M. Roper	Drag reduction of thin wings at supersonic speeds by the use of camber and twist. R. & M. 3132. July, 1957.
2	G. M. Roper	Some applications of the Lamé function solutions of the linearised supersonic flow equations. R. & M. 2865. August, 1951.
3	G. M. Roper	Calculation of the effect of camber and twist on the pressure distribution and drag on some curved plates at supersonic speeds. R. & M. 2794. September, 1950.
4	A. Robinson	Aerofoil theory of a flat delta wing at supersonic speeds. R. & M. 2548. September, 1946.
5	A. Robinson	Rotary derivatives of a delta wing at supersonic speeds. <i>J. R. Ae. Soc.</i> November, 1948.
6	E. W. Hobson	<i>Spherical and Ellipsoidal Harmonics.</i> Cambridge University Press.

APPENDIX I

The Functions $f_1, f_4, \dots, f_{31}; F_1, F_2, F_3, F_4; F_s$

$$\begin{aligned}
 f_1 = f_4 &= \{(2\kappa^2 - 1)E(\kappa) + (1 - \kappa^2)K(\kappa)\}/(2\kappa^2 E(\kappa)) \\
 f_5 &= 3\{(1 + \kappa^2)E(\kappa) - (1 - \kappa^2)K(\kappa)\}/(2\kappa^2 E(\kappa)) \\
 f_6 &= \{(2 + \kappa^2 - 3\kappa^4)K(\kappa) - (2 + 2\kappa^2 - 6\kappa^4)E(\kappa)\}/(2\kappa^4 E(\kappa)) \\
 f_7 &= \{(2 - 3\kappa^2 + \kappa^4)E(\kappa) - (2 - 4\kappa^2 + 2\kappa^4)K(\kappa)\}/(2\kappa^4 E(\kappa)) \\
 f_{10} &= \{(2 + 2\kappa^2 - 4\kappa^4)K(\kappa) - (2 + 3\kappa^2 - 8\kappa^4)E(\kappa)\}/(2\kappa^4 E(\kappa)) \\
 f_{11} &= 3\{(2 - 2\kappa^2 + 2\kappa^4)E(\kappa) - (2 - 3\kappa^2 + \kappa^4)K(\kappa)\}/(2\kappa^4 E(\kappa)) \\
 f_{12} &= \frac{\{(8 - \kappa^2 + 5\kappa^4 - 12\kappa^6)K(\kappa) - (8 + 3\kappa^2 + 7\kappa^4 - 24\kappa^6)E(\kappa)\}}{(6\kappa^6 E(\kappa))} \\
 f_{13} &= \frac{\{(8 - 11\kappa^2 + \kappa^4 + 2\kappa^6)E(\kappa) - (8 - 15\kappa^2 + 6\kappa^4 + \kappa^6)K(\kappa)\}}{(2\kappa^6 E(\kappa))} \\
 F_1 &= 1/(f_5 f_6 - 3f_4 f_7) \\
 F_2 &= 1/(f_{11} f_{12} - f_{10} f_{13}) \\
 f_{14} &= B_2 C_3 - B_3 C_2, \quad f_{15} = B_1 C_3 - B_3 C_1, \quad f_{16} = B_1 C_2 - B_2 C_1; \\
 f_{17} &= C_2 A_3 - C_3 A_2, \quad f_{18} = C_1 A_3 - C_3 A_1, \quad f_{19} = C_1 A_2 - C_2 A_1; \\
 f_{20} &= A_2 B_3 - A_3 B_2, \quad f_{21} = A_1 B_3 - A_3 B_1, \quad f_{22} = A_1 B_2 - A_2 B_1 \\
 F_3 &= 1/(A_1 f_{14} - A_2 f_{15} + A_3 f_{16}) \\
 &= 1/(B_1 f_{17} - B_2 f_{18} + B_3 f_{19}) \\
 &= 1/(C_1 f_{20} - C_2 f_{21} + C_3 f_{22}),
 \end{aligned}$$

where A_s, B_s, C_s ($s = 1, 2, 3$), ($n = 5$) are given in Appendix III,

$$\begin{aligned}
 f_{23} &= B_2 C_3 - B_3 C_2, \quad f_{24} = B_1 C_3 - B_3 C_1, \quad f_{25} = B_1 C_2 - B_2 C_1; \\
 f_{26} &= C_3 A_2 - C_2 A_3, \quad f_{27} = C_3 A_1 - C_1 A_3, \quad f_{28} = C_2 A_1 - C_1 A_2; \\
 f_{29} &= A_2 B_3 - A_3 B_2, \quad f_{30} = A_1 B_3 - A_3 B_1, \quad f_{31} = A_1 B_2 - A_2 B_1 \\
 F_4 &= 1/(A_1 f_{23} - A_2 f_{24} + A_3 f_{25}) \\
 &= -1/(B_1 f_{26} - B_2 f_{27} + B_3 f_{28}) \\
 &= 1/(C_1 f_{29} - C_2 f_{30} + C_3 f_{31}),
 \end{aligned}$$

where A_s, B_s, C_s , ($n = 6$), are given in Appendix III,

$$F_s = f_s + f_{s+1} + f_{s+2} \quad (s = 14, 17, 20, 23, 26, 29)$$

APPENDIX II

Equations for a_m, b_m for $n = 5$ and $n = 6$

$n = 5$

a_m ($m = 1, 2, 3$) are the roots of the cubic equation

$$27a_m^3 - Aa_m^2 + Ba_m - C = 0,$$

where

$$A = 60\kappa^2 + 42,$$

$$B = 32\kappa^4 + 68\kappa^2 + 16,$$

$$C = 2\kappa^2(12\kappa^2 + 8).$$

b_m is given by:

$$b_m = \kappa^2 a_m / (12\kappa^2 + 8 - 9a_m)$$

or

$$14b_m = 9a_m^2 - (8\kappa^2 + 6)a_m + 6\kappa^2$$

$n = 6$

a_m ($m = 1, 2, 3$) are the roots of the cubic equation

$$121a_m^3 - Aa_m^2 + Ba_m - C = 0,$$

where

$$A = 286\kappa^2 + 220,$$

$$B = 160\kappa^4 + 412\kappa^2 + 96,$$

$$C = 40\kappa^2(4\kappa^2 + 3).$$

b_m is given by:

$$18b_m = 11a_m^2 - (10\kappa^2 + 8)a_m + 10\kappa^2.$$

Numerical values of A, B, C for $n = 5$ and $n = 6$ are given in Table 6.

Numerical values of a_m, b_m for $n = 5$ and $n = 6$ are given in Tables 7 and 8.

TABLE 6

Numerical Values of A , B , C for $n = 5$ and $n = 6$

n	x^2	A	B	C	$\beta \tan \gamma$
5	0	42	16	0	1
	0.0975	47.85	22.9342	1.78815	0.95
	0.19	53.4	30.0752	3.9064	0.9
	0.2775	58.65	37.3342	6.28815	0.85
	0.36	63.6	44.6272	8.8704	0.8
	0.4375	68.25	51.875	11.59375	0.75
	0.48	70.8	56.0128	13.2096	0.7211
	0.51	72.6	59.0032	14.4024	0.7
	0.5211	73.266	60.12424672	14.85468504	0.692
	0.5775	76.65	65.9422	17.24415	0.65
	0.64	80.4	72.6272	20.0704	0.6
	0.6975	83.85	78.9982	22.83615	0.55
	0.75	87.0	85.0	25.5	0.5
	0.7975	89.85	90.5822	28.02415	0.45
	0.84	92.4	95.6992	30.3744	0.4
	0.8775	94.65	100.3102	32.52015	0.35
	0.91	96.6	104.3792	34.4344	0.3
	0.9375	98.25	107.875	36.09375	0.25
	0.96	99.6	110.7712	37.4784	0.2
	0.99	101.4	114.6832	39.3624	0.1
1	102	116	40	0	
6	0	220	96	0	1
	0.0975	247.885	137.691	13.221	0.95
	0.19	274.34	180.056	28.576	0.9
	0.2775	299.365	222.651	45.621	0.85
	0.36	322.96	265.056	63.936	0.8
	0.4375	345.125	306.875	83.125	0.75
	0.48	357.28	330.624	94.464	0.7211
	0.51	365.86	347.736	102.816	0.7
	0.5211	369.0346	354.1404336	105.9792336	0.692
	0.5775	385.165	387.291	122.661	0.65
	0.64	403.04	425.216	142.336	0.6
	0.6975	419.485	461.211	161.541	0.55
	0.75	434.50	495	180	0.5
	0.7975	448.085	526.331	197.461	0.45
	0.84	460.24	554.976	213.696	0.4
	0.8775	470.965	580.731	228.501	0.35
	0.91	480.26	603.416	241.696	0.3
	0.9375	488.125	622.875	253.125	0.25
	0.96	494.56	638.976	262.656	0.2
	0.99	503.14	660.696	275.616	0.1
1	506	668	280	0	

TABLE 7

Numerical values of a_m, b_m for the Lamé function

$$E_5^m(\mu) = (\mu^4 - a_m k^2 \mu^2 + b_m k^4) (|\mu^2 - k^2|)^{1/2}, \quad a_1 > a_2 > a_3$$

$\beta \tan \gamma$	a_1	b_1	a_2	b_2	a_3	b_3
1	8/9	8/63	2/3	0	0	0
0.95	0.956796079	0.16693222	0.719180036	0.02599562	0.0962461071	0.00113009
0.9	1.04214165	0.219830559	0.750701123	0.040478366	0.184935007	0.004078382
0.85	1.13389213	0.27970064	0.772420884	0.04895761	0.265909211	0.00825683
0.8	1.22583351	0.342757754	0.790825303	0.054722374	0.338896743	0.013161138
0.75	1.31512832	0.40695309	0.809112846	0.05931431	0.403536607	0.01835560
0.7211	1.36494874	0.444047822	0.820339242	0.061747862	0.436934233	0.021340775
0.7	1.40040828	0.471012478	0.829012542	0.063493551	0.459468070	0.023468573
0.692	1.41358329	0.481150961	0.832406215	0.06415205	0.467566044	0.02425546
0.65	1.48093637	0.53400059	0.851447494	0.06766379	0.506505024	0.02820305
0.6	1.55627204	0.595149908	0.876653373	0.072021763	0.544852372	0.032358470
0.55	1.62612869	0.653791468	0.904198007	0.076610959	0.575228861	0.03584600
0.5	1.69030748	0.709326001	0.933138349	0.081361742	0.598776383	0.038677271
0.45	1.74866391	0.761212108	0.962308994	0.08614014	0.616804867	0.04092785
0.4	1.80108932	0.808960628	0.990589561	0.090793564	0.630543347	0.042696632
0.35	1.84750020	0.85213296	1.01704871	0.09517990	0.641006638	0.04407852
0.3	1.88783150	0.890340489	1.04097597	0.099179843	0.648970305	0.045152604
0.25	1.92203256	0.92324594	1.06185459	0.10269854	0.655001740	0.045980015
0.2	1.95006379	0.950561911	1.07931970	0.105663261	0.659505402	0.046606606
0.1	1.98750392	0.987535117	1.10308120	0.109728783	0.664970421	0.047377337
0	2	1	10/9	1/9	2/3	1/21

TABLE 8

Numerical values of a_m, b_m for the Lamé function

$$E_6^m(\mu) = (\mu^5 - a_m k^2 \mu^3 + b_m k^4 \mu) (|\mu^2 - k^2|)^{1/2}, \quad a_1 > a_2 > a_3$$

$\beta \tan \gamma$	a_1	b_1	a_2	b_2	a_3	b_3
1	12/11	8/33	8/11	0	0	0
0.95	1.11887587	0.26132247	0.809057627	0.05077914	0.120702862	0.002886267
0.9	1.15982909	0.289718372	0.874637826	0.091999450	0.232805809	0.010633693
0.85	1.21509373	0.32907475	0.922717171	0.12212218	0.336280009	0.02197275
0.8	1.28140265	0.377647195	0.956639902	0.142763114	0.431048341	0.035759368
0.75	1.35346781	0.43202567	0.981848623	0.15716207	0.516956285	0.05096377
0.7211	1.39599192	0.464890625	0.994276109	0.163761143	0.562459232	0.060027005
0.7	1.42702890	0.489247094	1.00285836	0.168084959	0.593749101	0.066655817
0.692	1.43870185	0.49848906	1.00603985	0.16963808	0.605131022	0.06914629
0.65	1.49939626	0.54727206	1.02270524	0.17735674	0.661080324	0.08199543
0.6	1.56895165	0.604711017	1.04336009	0.186123208	0.718597325	0.096244544
0.55	1.63468796	0.66054440	1.06598281	0.19507890	0.766147383	0.10581905
0.5	1.69594127	0.713960834	1.09090912	0.204545469	0.804058681	0.119372468
0.45	1.75224811	0.76427468	1.11763757	0.21449950	0.833296141	0.12785007
0.4	1.80326987	0.810887699	1.14505777	0.224654601	0.855308710	0.134445557
0.35	1.84875105	0.85216033	1.17185516	0.23460108	0.871666535	0.13947899
0.3	1.88849468	0.890959705	1.19684203	0.243930032	0.883754224	0.143279976
0.25	1.92234768	0.92354643	1.21909627	0.25229751	0.892646959	0.14612576
0.2	1.95019137	0.95068567	1.23796155	0.259439639	0.899119837	0.148226231
0.1	1.98751176	0.987542914	1.26390395	0.269339135	0.906766096	0.150742175
0	2	1	14/11	3/11	10/11	5/33

APPENDIX III

Formulae for Calculating A_s, B_s, C_s for $n = 5, n = 6$

The constants A_s, B_s, C_s required for the calculation of $f_{14}, f_{15}, \dots, f_{22}$ are given by the formulae :
($s = 1, 2, 3$)

$$\begin{aligned} A_s &= \frac{(-1)^s}{5} \sum_{m=1}^3 \left[\left(\lambda_m \right)_s \left(1 - a_m + b_m \right) \left(\kappa^4 - a_m \kappa^2 - b_m \right) \mathcal{J}_m \right], \\ B_s &= \frac{(-1)^{s-1}}{3} (1 - \kappa^2) \sum_{m=1}^3 \left[\left(\lambda_m \right)_s \left(1 - a_m + b_m \right) \left(a_m \kappa^2 - 2b_m \right) \mathcal{J}_m \right], \\ C_s &= (-1)^s (1 - \kappa^2)^2 \sum_{m=1}^3 \left[\left(\lambda_m \right)_s \left(1 - a_m + b_m \right) b_m \mathcal{J}_m \right], \end{aligned} \quad (40)$$

where (See Appendix II, Ref. 1)*

$$\begin{aligned} \left(\lambda_1 \right)_1 &= \frac{1}{\kappa^4 \Delta} \left(a_2 b_3 - a_3 b_2 \right), \\ \left(\lambda_2 \right)_1 &= \frac{1}{\kappa^4 \Delta} \left(a_3 b_1 - a_1 b_3 \right), \\ \left(\lambda_3 \right)_1 &= \frac{1}{\kappa^4 \Delta} \left(a_1 b_2 - a_2 b_1 \right), \\ \left(\lambda_1 \right)_2 &= \frac{1}{\kappa^2 (1 - \kappa^2) \Delta} \left[b_2 - b_3 + \frac{1}{\kappa^2} \left(a_2 b_3 - a_3 b_2 \right) \right], \text{ etc.} \\ \left(\lambda_1 \right)_3 &= \frac{1}{(1 - \kappa^2)^2 \Delta} \left[\frac{1}{\kappa^4} \left(a_2 b_3 - a_3 b_2 \right) + \frac{2}{\kappa^2} \left(b_2 - b_3 \right) - \left(a_2 - a_3 \right) \right], \text{ etc.} \\ \Delta &= a_2 b_3 - a_3 b_2 + a_3 b_1 - a_1 b_3 + a_1 b_2 - a_2 b_1; \end{aligned} \quad (41)$$

a_m, b_m are given in Appendix II, and

$$\begin{aligned} \mathcal{J}_m &= \frac{(1 - \kappa^2)(1 - a_m + b_m)}{a_m^2 - 4b_m} \left[\frac{1}{2} \left\{ \frac{a_m}{\kappa^2 b_m} + \frac{2\kappa^2 - a_m}{(1 - \kappa^2)^2 \kappa^2 (\kappa^4 - a_m \kappa^2 + b_m)} \right. \right. \\ &\quad - 3 \left(\frac{2 - 2a_m + a_m^2 - 2b_m}{(1 - \kappa^2)(1 - a_m + b_m)^2} \right) + \frac{\kappa^2 - 2}{(1 - \kappa^2)^2} \left(\frac{2 - a_m}{1 - a_m + b_m} \right) + \\ &\quad \left. \left. + \frac{4}{(1 - \kappa^2)(1 - a_m + b_m)} \right\} - \frac{K(\kappa)}{E(\kappa)} \left\{ 2 \left(\frac{a_m - 1}{b_m(1 - a_m + b_m)} \right) + \right. \right. \\ &\quad \left. \left. + \frac{\frac{1}{2} \left[a_m^2 - 2b_m - 2a_m(a_m^2 - b_m) + a_m^4 + 4a_m^2 b_m - 14b_m^2 - 4a_m b_m(a_m^2 - 3b_m) \right]}{b_m^2 (1 - a_m + b_m)^2} \right] \right\} \right]. \end{aligned} \quad (42)$$

* $(\lambda_m)_s$ here replaces the $(k^{2s+2} \lambda_m^s)$ used in Ref. 1.

$\kappa^2 = 1 - \beta^2 \tan^2 \gamma$, and $K(\kappa)$, $E(\kappa)$ are complete elliptic integrals of the first and second kind respectively, of modulus κ .

The constants A_s , B_s , C_s required for the calculation of f_{23} , f_{24} , \dots , f_{31} are given by the formulae: ($s = 1, 2, 3$)

$$\left. \begin{aligned} A_s &= \frac{(-1)^s}{6} \sum_{m=1}^3 \left[\left(\lambda_m \right)_s \left(1 - a_m + b_m \right) \left(\kappa^4 - a_m \kappa^2 + b_m \right) \mathcal{J}_m \right], \\ B_s &= \frac{(-1)^{s-1}}{4} (1 - \kappa^2) \sum_{m=1}^3 \left[\left(\lambda_m \right)_s \left(1 - a_m + b_m \right) \left(a_m \kappa^2 - 2b_m \right) \mathcal{J}_m \right], \\ C_s &= \frac{(-1)^s}{2} (1 - \kappa^2)^2 \sum_{m=1}^3 \left[\left(\lambda_m \right)_s \left(1 - a_m + b_m \right) b_m \mathcal{J}_m \right], \end{aligned} \right\} \quad (43)$$

where $(\lambda_m)_s$ is given by formulae (41), a_m , b_m are given in Appendix II, and

$$\begin{aligned} \mathcal{J}_m &= \frac{(1 - \kappa^2)(1 - a_m + b_m)}{(d_1 - d_2)_m^2} \sum_{r=1}^2 \left[\left\{ \frac{1}{\kappa^2 d_r^2} + \frac{1}{2d_r^2 (\kappa^2 - d_r)(1 - d_r)^2} - \right. \right. \\ &\quad \left. \left. - \frac{1}{(1 - \kappa^2)(1 - d_r)^2} \right\}_m + \left\{ \frac{3\kappa^2(2d_r - 1) - 2d_r(1 - d_r)^2}{2\kappa^2 d_r^3 (1 - d_r)^2} \right\}_m \frac{K(\kappa)}{E(\kappa)} + \right. \\ &\quad \left. + \frac{1}{2d_r} \left(7 - \frac{3}{1 - d_r} - \frac{\kappa^2}{\kappa^2 - d_r} \right)_m \left\{ \frac{\kappa^2(1 - 2d_r) - (1 - d_r)}{\kappa^2 d_r (1 - d_r)(1 - \kappa^2)} \right\}_m + \right. \\ &\quad \left. + \left\{ \frac{\kappa^2 + d_r(1 - d_r)}{\kappa^2 d_r^2 (1 - d_r)} \right\}_m \frac{K(\kappa)}{E(\kappa)} \right]; \end{aligned} \quad (44)$$

and, for each value of m , d_1 , d_2 are the roots of the equation

$$D^2 - a_m D + b_m = 0.$$

APPENDIX IV

Formulae for the Evaluation of Certain Integrals

The following integrals occur in calculations for the triangular wing:

$$I_{2m,n} \equiv k \int_0^{1/k} \int_{ky}^1 \frac{k^{2m} y^{2m} x^n}{(x^2 - k^2 y^2)^{1/2}} dx dy = \frac{\pi(2m)!}{2^{2m+1}(2m+n+1)(m!)^2}$$

$$I_{2m+1,n} \equiv k \int_0^{1/k} \int_{ky}^1 \frac{k^{2m+1} y^{2m+1} x^n}{(x^2 - k^2 y^2)^{1/2}} dx dy = \frac{2^{2m}(m!)^2}{(2m+n+2)(2m+1)!}$$

$$L_{2m,n} \equiv k \int_0^{1/k} \int_{ky}^1 \frac{(ky)^{2m} x^n (x^2 - k^2 y^2)^{1/2}}{dx dy} = \frac{\pi(2m)!(2m+2)}{2^{2m+3}(2m+n+3)[(m+1)!]^2}$$

$$L_{2m+1,n} \equiv k \int_0^{1/k} \int_{ky}^1 \frac{(ky)^{2m+1} x^n (x^2 - k^2 y^2)^{1/2}}{dx dy} = \frac{2^{2m}(m!)^2(2m+2)}{(2m+n+4)(2m+3)!}$$

Reduction formulae

$$(2m+n+1)I_{2m,n} - (2m+n)I_{2m,n-1} = 0$$

$$2m(2m+n+1)I_{2m,n} - (2m-1)(2m+n-1)I_{2m-2,n} = 0$$

$$(2m+n+2)I_{2m+1,n} - (2m+n+1)I_{2m+1,n-1} = 0$$

$$(2m+1)(2m+n+2)I_{2m+1,n} - 2m(2m+n)I_{2m-1,n} = 0$$

$$(2m+n+3)L_{2m,n} - (2m+n+2)L_{2m,n-1} = 0$$

$$2(m+1)(2m+n+3)L_{2m,n} - (2m-1)(2m+n+1)L_{2m-2,n} = 0$$

$$(2m+n+4)L_{2m+1,n} - (2m+n+3)L_{2m+1,n-1} = 0$$

$$(2m+3)(2m+n+4)L_{2m+1,n} - 2m(2m+n+2)L_{2m-1,n} = 0.$$

Also:

$$L_{2m,n} = I_{2m,n+2} - I_{2m+2,n}$$

$$L_{2m+1,n} = I_{2m+1,n+2} - I_{2m+3,n}$$

APPENDIX V

Triangular Wing with No Leading-Edge Load
 Numerical Values for $d_r, d_{r,s}$. ($d_{r,s} \equiv 2d_r$)

$$\beta \tan \gamma = 0.614, \quad \kappa^2 = 0.6231$$

r	d_r	$d_{a,r}$	$d_{b,r}$	$d_{c,r}$	$d_{d,r}$	$d_{e,r}$	$d_{f,r}$
a	1.207333	2.414667	2.597448	2.737294	2.075978	2.845257	2.144872
b	1.421814	2.597448	2.843628	3.038806	2.286968	3.194448	2.390097
c	1.642218	2.737294	3.038806	3.284435	2.457858	3.485107	2.595555
d	1.761130	2.075978	2.286968	2.457858	3.522260	2.733143	3.740358
e	1.863598	2.845250	3.194439	3.485107	2.597721	3.727195	2.901664
f	2.000332	2.144872	2.390097	2.595555	3.740358	2.901664	4.000664

$$\beta \tan \gamma = 0.3, \quad \kappa^2 = 0.91$$

r	d_r	$d_{a,r}$	$d_{b,r}$	$d_{c,r}$	$d_{d,r}$	$d_{e,r}$	$d_{f,r}$
a	0.896865	1.793729	1.884127	1.957296	1.480487	2.017396	1.507162
b	1.001545	1.884127	2.003090	2.101986	1.601042	2.185025	1.646064
c	1.112449	1.957296	2.101986	2.224899	1.702337	2.329978	1.765171
d	1.099744	1.480487	1.601042	1.702337	2.199488	1.788382	2.318303
e	1.227887	2.017396	2.185025	2.329978	1.788382	2.455773	1.867502
f	1.228749	1.507162	1.646064	1.765171	2.318303	1.867502	2.457497
g	0.882011	1.747990	1.809823	1.858327	1.241938	1.949171	

APPENDIX VI

Formulae for Calculating the Coefficients a_s , or b_s , and the Zeros c_r , or d_r , of Standard Lamé Functions of the M Class for any Value of n

The standard Lamé functions of the M class can be written in the forms:

$$E_s(\mu) = (|\mu^2 - k^2|)^{1/2} \sum_{s=0}^{(n-1)/2} \left[(-1)^s a_s k^{2s} \mu^{n-2s-1} \right]$$

$$\equiv (|\mu^2 - k^2|)^{1/2} \prod_{r=1}^{(n-1)/2} (\mu^2 - c_r k^2) \quad \text{if } n \text{ is odd,}$$

and

$$E_s(\mu) = (|\mu^2 - k^2|)^{1/2} \sum_{s=0}^{(n-2)/2} \left[(-1)^s b_s k^{2s} \mu^{n-2s-1} \right]$$

$$\equiv (|\mu^2 - k^2|)^{1/2} \mu \prod_{r=1}^{(n-2)/2} (\mu^2 - d_r k^2) \quad \text{if } n \text{ is even,}$$

where $a_0 = b_0 = 1$, and a_s, b_s, c_r, d_r are all real and positive.

It can be shown that the Lamé coefficients a_s, b_s and the zeros c_r, d_r are given by the following relations:

$$a_0 = 1$$

$$2(2n-1)a_1 = n^2 \kappa^2 + (n-1)^2 - \lambda,$$

$$2s(2n-2s+1)a_s = [(n-2s+2)^2 \kappa^2 + (n-2s+1)^2 - \lambda] a_{s-1} +$$

$$+ (n-2s+3)(n-2s+2) \kappa^2 a_{s-2}, \quad s = 2, 3, \dots, (n-1)/2,$$

$$0 = (\kappa^2 - \lambda) a_{(n-1)/2} + 2\kappa^2 a_{(n-3)/2},$$

where λ is an unknown quantity proportional to $1 + \kappa^2$. These $(n+1)/2$ equations give the $(n+1)/2$ values of λ and of each of the $(n-1)/2$ quantities a_s for any value of κ^2 .

c_r are the roots of the equation

$$\sum_{s=0}^{(n-1)/2} \left[(-1)^s a_s C^{n-2s-1} \right] = 0.$$

$$b_0 = 1$$

$$2(2n-1)b_1 = n^2 \kappa^2 + (n-1)^2 - \lambda,$$

$$2s(2n-2s+1)b_s = [(n-2s+2)^2 \kappa^2 + (n-2s+1)^2 - \lambda] b_{s-1} +$$

$$+ (n-2s+3)(n-2s+2) \kappa^2 b_{s-2}, \quad s = 2, 3, \dots, (n-2)/2,$$

$$0 = (4\kappa^2 + 1 - \lambda) b_{(n-2)/2} + 6\kappa^2 b_{(n-4)/2}.$$

These $n/2$ equations give the $n/2$ values of λ and of each of the $(n - 2)/2$ quantities b_s for the value of κ^2 .

d_r are the roots of the equation

$$\sum_{s=0}^{(n-2)/2} \left[(-1)^s b_s D^{n-2s-1} \right] = 0.$$

c_r , d_r can also be calculated from equations (18a) and (18b), and a_s , b_s from equations (23) given in Section 6.

TABLES 9 to 14

All Forces are Normalised by Dividing by $(\pi\rho V^2 c^2)/(k^2 E(\kappa))$

TABLE 9

Formulae for the Total Lift on 'Basic' Triangular Surfaces

r	z_r	L_r	Type of surface
1	$-\delta x$	δ	Camber
2	$-\frac{\delta}{c} x^2$	$\frac{\delta}{f_1}$	
3	$-\frac{\delta}{c^2} x^3$	$\frac{3}{4} \delta F_1(4f_5 - 3f_7)$	
4	$-\frac{\delta}{c^3} x^4$	$\delta F_2(4f_{11} - 3f_{13})$	
8	$-\frac{\delta}{c^4} x^5$	$\frac{1}{8} \delta F_3(8f_{14} + 2f_{15} + f_{16})$	
11	$-\frac{\delta}{c^5} x^6$	$\frac{1}{8} \delta F_4(8f_{23} + 2f_{24} + f_{25})$	
2a	$-\frac{\delta}{c} x ky $	$\frac{\delta E(\kappa)}{\pi} \left(\frac{2}{3} - \frac{1}{f_1} \right)$	Twist
5	$-\frac{\delta}{c^2} k^2 y^2 x$	$\frac{3}{4} \delta F_1(4f_4 - f_6)$	
6	$-\frac{\delta}{c^3} k^2 y^2 x^2$	$\frac{1}{2} \delta F_2(4f_{10} - 3f_{12})$	Camber and twist
9	$-\frac{\delta}{c^4} k^2 y^2 x^3$	$-\frac{1}{8} \delta F_3(8f_{17} + 2f_{18} + f_{19})$	
12	$-\frac{\delta}{c^5} k^2 y^2 x^4$	$\frac{1}{8} \delta F_4(8f_{26} + 2f_{27} + f_{28})$	
10	$-\frac{\delta}{c^4} k^4 y^4 x$	$\frac{1}{8} \delta F_3(8f_{20} + 2f_{21} + f_{22})$	Twist
13	$-\frac{\delta}{c^5} k^4 y^4 x^2$	$\frac{1}{8} \delta F_4(8f_{29} + 2f_{30} + f_{31})$	Camber and twist

TABLE 10

*Formulae for the Total Lift on Basic 'No singularity' Triangular Surfaces
(x, y, z are Measured in Chord Lengths)*

r	z_r	L_r
a	$-\delta(f_4x^3 - f_5k^2y^2x)$	$\frac{3}{4}\delta$
b	$-\delta(f_{10}x^4 - 2f_{11}k^2y^2x^2)$	3δ
c	$+\delta(F_{17}x^5 + F_{14}k^2y^2x^3)$	$-(F_{17}L_8 + F_{14}L_0)$
d	$-\delta(F_{20}k^2y^2x^3 + F_{17}k^4y^4x)$	$F_{20}L_9 + F_{17}L_{10}$
e	$-\delta(F_{26}x^6 - F_{23}k^2y^2x^4)$	$F_{26}L_{11} - F_{23}L_{12}$
f	$-\delta(F_{29}k^2y^2x^4 - F_{26}k^4y^4x^2)$	$F_{29}L_{12} - F_{26}L_{13}$
g	$-\delta(x^2 - \frac{\pi}{E(\kappa)}x ky)$	$\frac{2}{3}\delta$

TABLE 11

*Formulae for the Drag Component, D_r , of the Pressure Integral for Triangular Surfaces
(Formulae for $r = 1$ to 10 are Given in Table 4, Ref. 1)*

r	D_r
8	$3\delta L_8$
9	$-\frac{3}{80} \delta^2 F_3 (16f_{17} + 8f_{18} + 5f_{19})$
10	$\frac{1}{128} \delta^2 F_3 (16f_{20} + 10f_{21} + 7f_{22})$
11	$\frac{7}{2} \delta L_{11}$
12	$\frac{3}{64} \delta^2 F_4 (16f_{26} + 8f_{27} + 5f_{28})$
13	$\frac{11}{768} \delta^2 F_4 (16f_{29} + 10f_{30} + 7f_{31})$

TABLE 12

Formulae for $d_r = D_r/L_r^2$ for Basic 'No singularity' Triangular Surfaces

r	d_r
a	$\frac{2}{9}(12f_4 - f_5)$
b	$\frac{1}{36}(30f_{10} - 7f_{11})$
c	$\frac{1}{L_c^2} [F_{17}^2 D_8 + F_{14}^2 D_9 + F_{17} F_{14} D_{8,9}]$
d	$\frac{1}{L_d^2} [F_{20}^2 D_9 + F_{17}^2 D_{10} + F_{20} F_{17} D_{9,10}]$
e	$\frac{1}{L_e^2} [F_{26}^2 D_{11} + F_{23}^2 D_{12} - F_{26} F_{23} D_{11,12}]$
f	$\frac{1}{L_f^2} [F_{29}^2 D_{12} + F_{26}^2 D_{13} - F_{29} F_{26} D_{12,13}]$
g	$\frac{3}{4} \left[3 - \frac{2}{E(z)} \right]$

TABLE 13

Formulae for the 'Interference' Pressure Integral for Triangular Surfaces

($D_{r,s} = D_{s,r}$ is the 'interference' pressure integral for the two surfaces give by z_r, z_s)
 Formulae for $r = 1$ to 10, $s = 1$ to 10 are given in Table 6, Ref. 1

r, s	$D_{r,s}$
1, 11	$\delta \left(\frac{12}{7} \delta + L_{11} \right)$
1, 12	$\delta \left(\frac{4}{7} \delta + L_{12} \right)$
1, 13	$\delta \left(\frac{3}{14} \delta + L_{13} \right)$
2, 11	$\delta \left(\frac{9}{4f_1} \delta + \frac{7}{4} L_{11} \right)$
2, 12	$\delta \left(\frac{5}{8f_1} \delta + \frac{7}{4} L_{12} \right)$
2, 13	$\delta \left(\frac{7}{32f_1} \delta + \frac{7}{4} L_{13} \right)$
3, 11	$\delta \left(\frac{8}{3} L_3 + \frac{7}{3} L_{11} \right)$
3, 12	$\delta \left[\delta F_1(2f_5 - f_7) + \frac{7}{3} L_{12} \right]$
3, 13	$\delta \left[\frac{\delta}{12} F_1(8f_5 - 3f_7) + \frac{7}{3} L_{13} \right]$
4, 11	$\delta \left(3L_4 + \frac{14}{5} L_{11} \right)$
4, 12	$\delta \left[\frac{7}{5} \delta F_2(2f_{11} - f_{13}) + \frac{14}{5} L_{12} \right]$
4, 13	$\delta \left[\frac{9}{80} \delta F_2(8f_{11} - 3f_{13}) + \frac{14}{5} L_{13} \right]$
5, 11	$\delta \left[\frac{8}{3} L_5 + \frac{\delta}{64} F_4(16f_{23} + 8f_{24} + 5f_{25}) \right]$
5, 12	$\delta^2 \left[\frac{1}{3} F_1(6f_4 - f_6) + \frac{1}{64} F_4(16f_{26} + 8f_{27} + 5f_{28}) \right]$

TABLE 13—continued

r, s	$D_{r,s}$
5, 13	$\delta^2 \left[\frac{1}{12} F_1(8f_4 - f_6) + \frac{1}{64} F_4(16f_{29} + 8f_{30} + 5f_{31}) \right]$
6, 11	$\delta \left[3L_6 + \frac{9}{320} \delta F_4(16f_{23} + 8f_{24} + 5f_{25}) \right]$
6, 12	$\delta^2 \left[\frac{7}{10} F_2(2f_{10} - f_{12}) + \frac{9}{320} F_4(16f_{26} + 8f_{27} + 5f_{28}) \right]$
6, 13	$\frac{9}{320} \delta^2 \left[2F_2(8f_{10} - 3f_{12}) + F_4(16f_{29} + 8f_{30} + 5f_{31}) \right]$
8, 11	$\frac{\delta}{11} (36L_8 + 35L_{11})$
8, 12	$\frac{\delta}{11} \left[\frac{\delta}{2} F_3(16f_{14} + 8f_{15} + 5f_{16}) + 35L_{12} \right]$
8, 13	$\frac{5}{11} \delta \left[\frac{\delta}{32} F_3(16f_{14} + 10f_{15} + 7f_{16}) + 7L_{13} \right]$
9, 11	$\frac{9}{11} \delta \left[4L_9 + \frac{3}{34} \delta F_4(16f_{23} + 8f_{24} + 5f_{25}) \right]$
9, 12	$\frac{\delta^2}{22} \left[\frac{27}{32} F_4(16f_{26} + 8f_{27} + 5f_{28}) - F_3(16f_{17} + 8f_{18} + 5f_{19}) \right]$
9, 13	$\frac{\delta^2}{704} \left[27F_4(16f_{29} + 8f_{30} + 5f_{31}) - 10F_3(16f_{17} + 10f_{18} + 7f_{19}) \right]$
10, 11	$\delta \left[\frac{36}{11} L_{10} + \frac{\delta}{128} F_4(16f_{23} + 10f_{24} + 7f_{25}) \right]$
10, 12	$\delta^2 \left[\frac{1}{22} F_3(16f_{20} + 8f_{21} + 5f_{22}) + \frac{1}{128} F_4(16f_{26} + 10f_{27} + 7f_{28}) \right]$
10, 13	$\frac{\delta^2}{32} \left[\frac{5}{11} F_3(16f_{20} + 10f_{21} + 7f_{22}) + \frac{1}{4} F_4(16f_{29} + 10f_{30} + 7f_{31}) \right]$
11, 12	$\delta \left[\frac{3}{64} \delta F_4(16f_{23} + 8f_{24} + 5f_{25}) + \frac{7}{2} L_{12} \right]$
11, 13	$\delta \left[\frac{11}{768} \delta F_4(16f_{23} + 10f_{24} + 7f_{25}) + \frac{7}{2} L_{13} \right]$
12, 13	$\frac{\delta^2}{64} \left[\frac{11}{12} F_4(16f_{26} + 10f_{27} + 7f_{28}) + 3F_4(16f_{29} + 8f_{30} + 5f_{31}) \right]$

TABLE 14

Formulae for $d_{r,s} = D_{r,s}(L_r L_s)$ for Basic 'No singularity' Triangular Surfaces

r, s	$d_{r,s}$
a, b	$\frac{1}{L_a L_b} (f_4 \cdot f_{10} D_{3,4} + f_5 \cdot 2f_{11} D_{5,6} - f_4 \cdot 2f_{11} D_{3,6} - f_5 \cdot f_{10} D_{4,5})$
a, c	$\frac{1}{L_a L_c} (-f_4 \cdot F_{17} D_{3,8} + f_5 \cdot F_{14} D_{5,9} - f_4 \cdot F_{14} D_{3,9} + f_5 \cdot F_{17} D_{5,8})$
a, d	$\frac{1}{L_a L_d} (f_4 \cdot F_{20} D_{3,9} - f_5 \cdot F_{17} D_{5,10} + f_4 \cdot F_{17} D_{3,10} - f_5 \cdot F_{20} D_{5,9})$
a, e	$\frac{1}{L_a L_e} (f_4 \cdot F_{26} D_{3,11} + f_5 \cdot F_{23} D_{5,12} - f_4 \cdot F_{23} D_{3,12} - f_5 \cdot F_{26} D_{5,11})$
a, f	$\frac{1}{L_a L_f} (f_4 \cdot F_{29} D_{3,12} + f_5 \cdot F_{26} D_{5,13} - f_4 \cdot F_{26} D_{3,13} - f_5 \cdot F_{29} D_{5,12})$
b, c	$\frac{1}{L_b L_c} (-f_{10} \cdot F_{17} D_{4,8} + 2f_{11} \cdot F_{14} D_{6,9} - f_{10} \cdot F_{14} D_{4,9} + 2f_{11} \cdot F_{17} D_{6,8})$
b, d	$\frac{1}{L_b L_d} (f_{10} \cdot F_{20} D_{4,9} - 2f_{11} \cdot F_{17} D_{6,10} + f_{10} \cdot F_{17} D_{4,10} - 2f_{11} \cdot F_{20} D_{6,9})$
b, e	$\frac{1}{L_b L_e} (f_{10} \cdot F_{26} D_{4,11} + 2f_{11} \cdot F_{23} D_{6,12} - f_{10} \cdot F_{23} D_{4,12} - 2f_{11} \cdot F_{26} D_{6,11})$
b, f	$\frac{1}{L_b L_f} (f_{10} \cdot F_{29} D_{4,12} + 2f_{11} \cdot F_{26} D_{6,13} - f_{10} \cdot F_{26} D_{4,13} - 2f_{11} \cdot F_{29} D_{6,12})$
c, d	$\frac{-1}{L_c L_d} (F_{17} \cdot F_{20} D_{8,9} + F_{14} \cdot F_{17} D_{9,10} + F_{17}^2 D_{8,10} + 2F_{14} \cdot F_{20} D_9)$
c, e	$\frac{1}{L_c L_e} (-F_{17} \cdot F_{26} D_{8,11} + F_{14} \cdot F_{23} D_{9,12} + F_{17} \cdot F_{23} D_{8,12} - F_{14} \cdot F_{26} D_{9,11})$
c, f	$\frac{1}{L_c L_f} (-F_{17} \cdot F_{29} D_{8,12} + F_{14} \cdot F_{26} D_{9,13} + F_{17} \cdot F_{26} D_{8,13} - F_{14} \cdot F_{29} D_{9,12})$
d, e	$\frac{1}{L_d L_e} (F_{20} \cdot F_{26} D_{9,11} - F_{17} \cdot F_{23} D_{10,12} - F_{20} \cdot F_{23} D_{9,12} + F_{17} \cdot F_{26} D_{10,11})$
d, f	$\frac{1}{L_d L_f} (F_{20} \cdot F_{29} D_{9,12} - F_{17} \cdot F_{26} D_{10,13} - F_{20} \cdot F_{26} D_{9,13} + F_{17} \cdot F_{29} D_{10,12})$
e, f	$\frac{1}{L_e L_f} (F_{26} \cdot F_{29} D_{11,12} + F_{23} \cdot F_{26} D_{12,13} - F_{26}^2 D_{11,13} - 2F_{23} \cdot F_{29} D_{12})$

TABLE 14—continued

r, s	$d_{r,s}$
a, g	$\frac{1}{5} \left[12f_4 - f_5 + 12 - \frac{8}{E(\kappa)} \right]$
b, g	$\frac{1}{30} \left[20f_{10} - 5f_{11} + 75 - \frac{48}{E(\kappa)} \right]$
c, g	$\frac{3}{2L_c} \left[-\frac{1}{14} (20F_{17} + 3F_{14}) + \frac{F_3}{14} \left\{ F_{14} (16f_{17} - 2f_{18} - 5f_{19}) - \right. \right.$ $- F_{17} (16f_{14} - 2f_{15} - 5f_{16}) \left. \right\} - \frac{4}{105} \frac{F_3}{E(\kappa)} \left\{ F_{14} (20f_{17} - f_{18} - 7f_{19}) - \right.$ $\left. \left. - F_{17} (20f_{14} - f_{15} - 7f_{16}) \right\} \right]$
d, g	$\frac{3}{2L_d} \left[\frac{1}{28} (6F_{20} + F_{17}) + \frac{F_3}{14} \left\{ F_{17} (16f_{20} - 2f_{21} - 5f_{22}) - F_{20} (16f_{17} - \right. \right.$ $- 2f_{18} - 5f_{19}) \left. \right\} - \frac{4}{105} \frac{F_3}{E(\kappa)} \left\{ F_{17} (20f_{20} - f_{21} - 7f_{22}) - \right.$ $\left. \left. - F_{20} (20f_{17} - f_{18} - 7f_{19}) \right\} \right]$
e, g	$\frac{3}{2L_e} \left[\frac{1}{4} (6F_{26} - F_{23}) + \frac{F_4}{32} \left\{ F_{26} (40f_{23} - 2f_{24} - 9f_{25}) - F_{23} (40f_{26} - \right. \right.$ $- 2f_{27} - 9f_{28}) \left. \right\} - \frac{F_4}{210E(\kappa)} \left\{ F_{26} (175f_{23} + 7f_{24} - 41f_{25}) - \right.$ $\left. \left. - F_{23} (175f_{26} + 7f_{27} - 41f_{28}) \right\} \right]$
f, g	$\frac{3}{2L_f} \left[\frac{1}{32} (8F_{29} - F_{26}) + \frac{F_4}{32} \left\{ F_{29} (40f_{26} - 2f_{27} - 9f_{28}) - \right. \right.$ $- F_{26} (40f_{29} - 2f_{30} - 9f_{31}) \left. \right\} - \frac{F_4}{210E(\kappa)} \left\{ F_{29} (175f_{26} + 7f_{27} - 41f_{28}) - \right.$ $\left. \left. - F_{26} (175f_{29} + 7f_{30} - 41f_{31}) \right\} \right]$

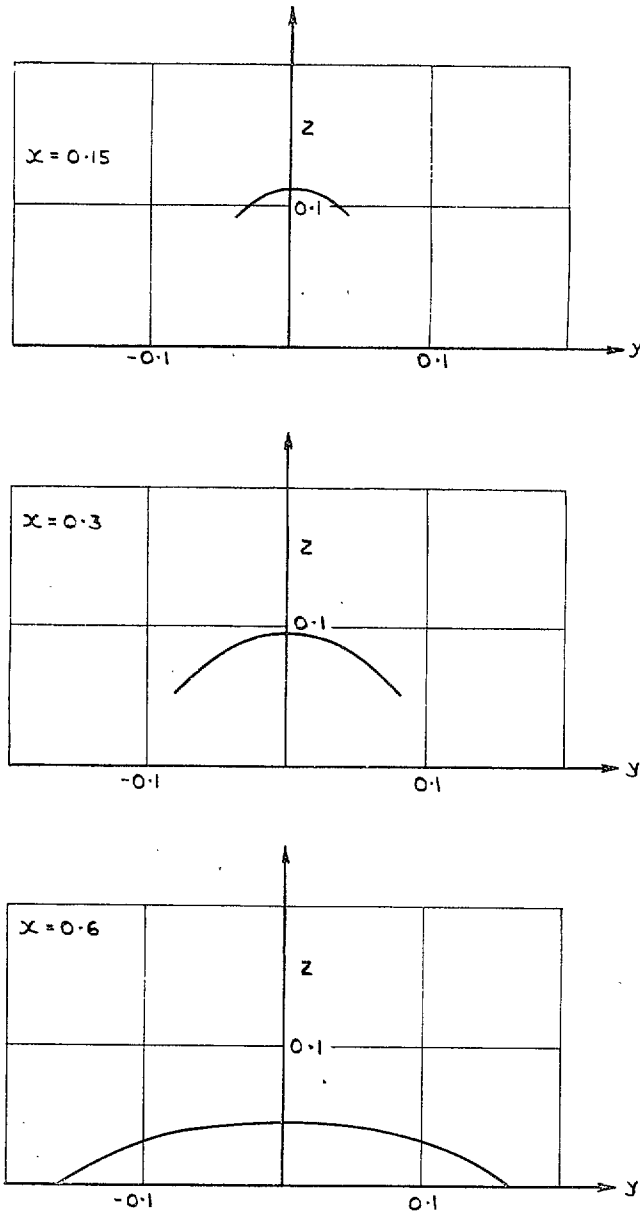


FIG. 1. Shape of camber surface of Wing 1.
 (Spanwise sections), $\gamma = 15$ deg., designed for minimum C_D/C_L^2 , with no leading-edge pressure singularities,
 at $M = 2.5$, $C_{L0} = 0.1$ (x, y, z are measured in root chord lengths, $z = 0$ at the trailing edge).

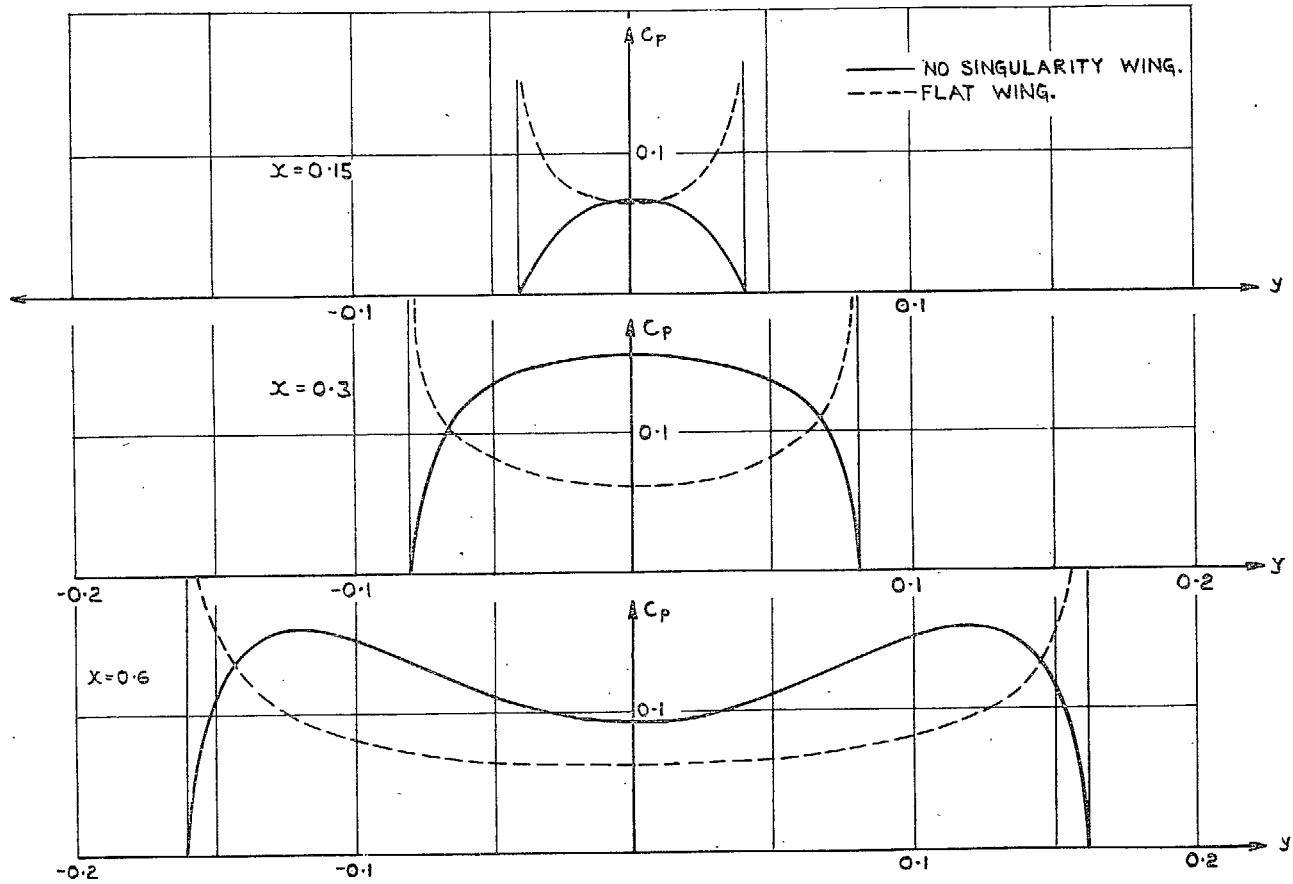


FIG. 2. Spanwise variation of loading coefficient, C_p , of Wing 1 at $M = 2.5$, $C_{L_0} = 0.1$.

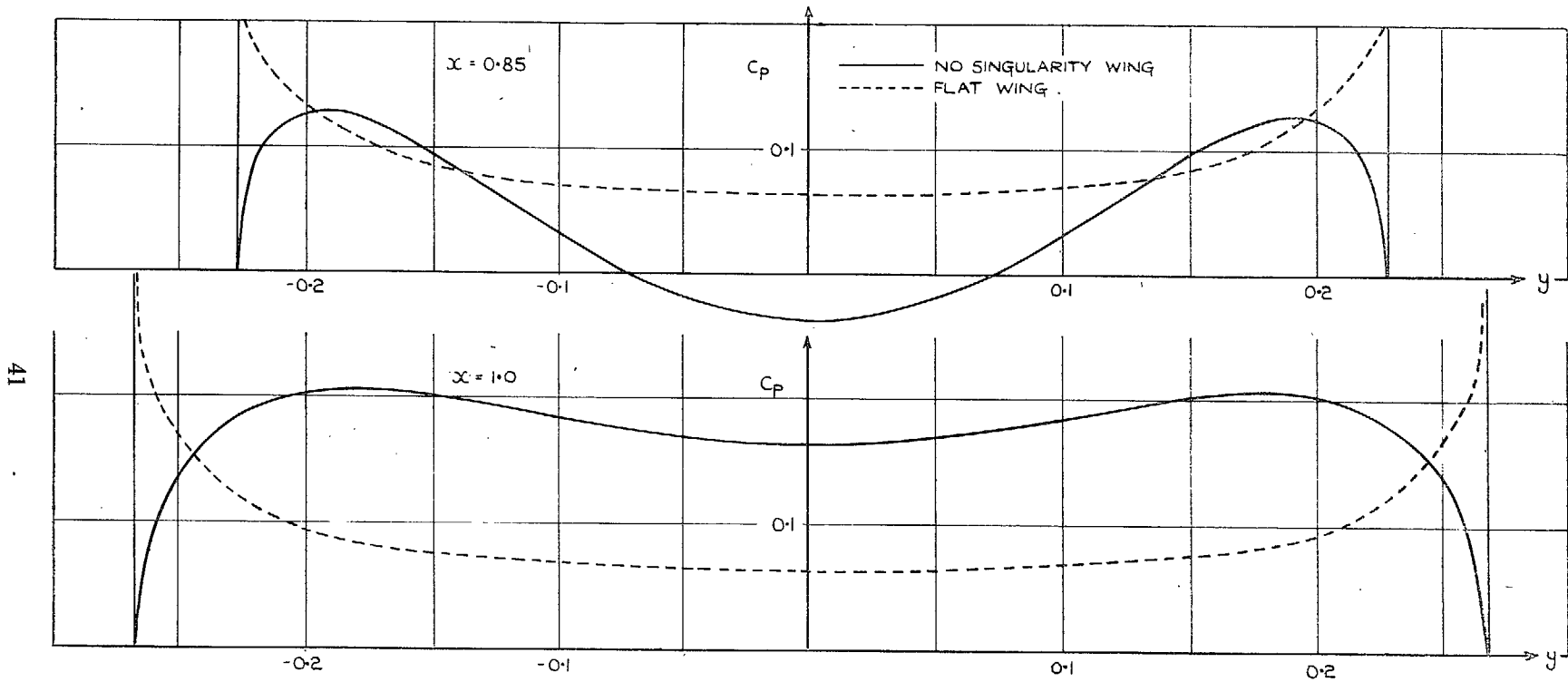


FIG. 2—continued. Spanwise variation of loading coefficient of Wing 1 at $M = 2.5$, $C_{L0} = 0.1$.

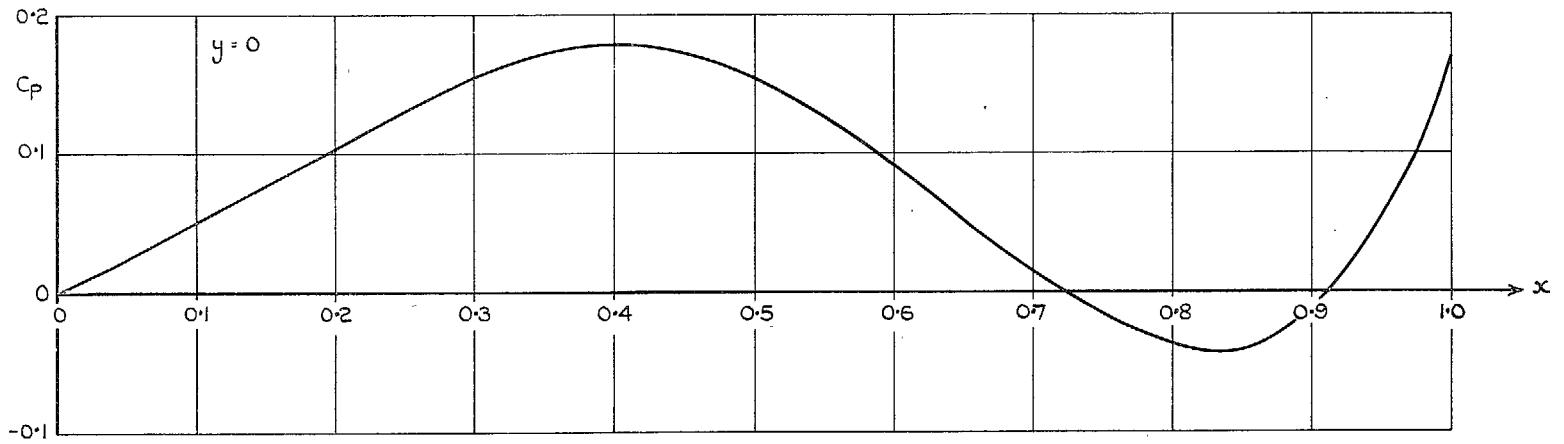


FIG. 3. Variation of loading coefficient along the root chord of Wing 1, at $M = 2.5$, $C_{L_0} = 0.1$.

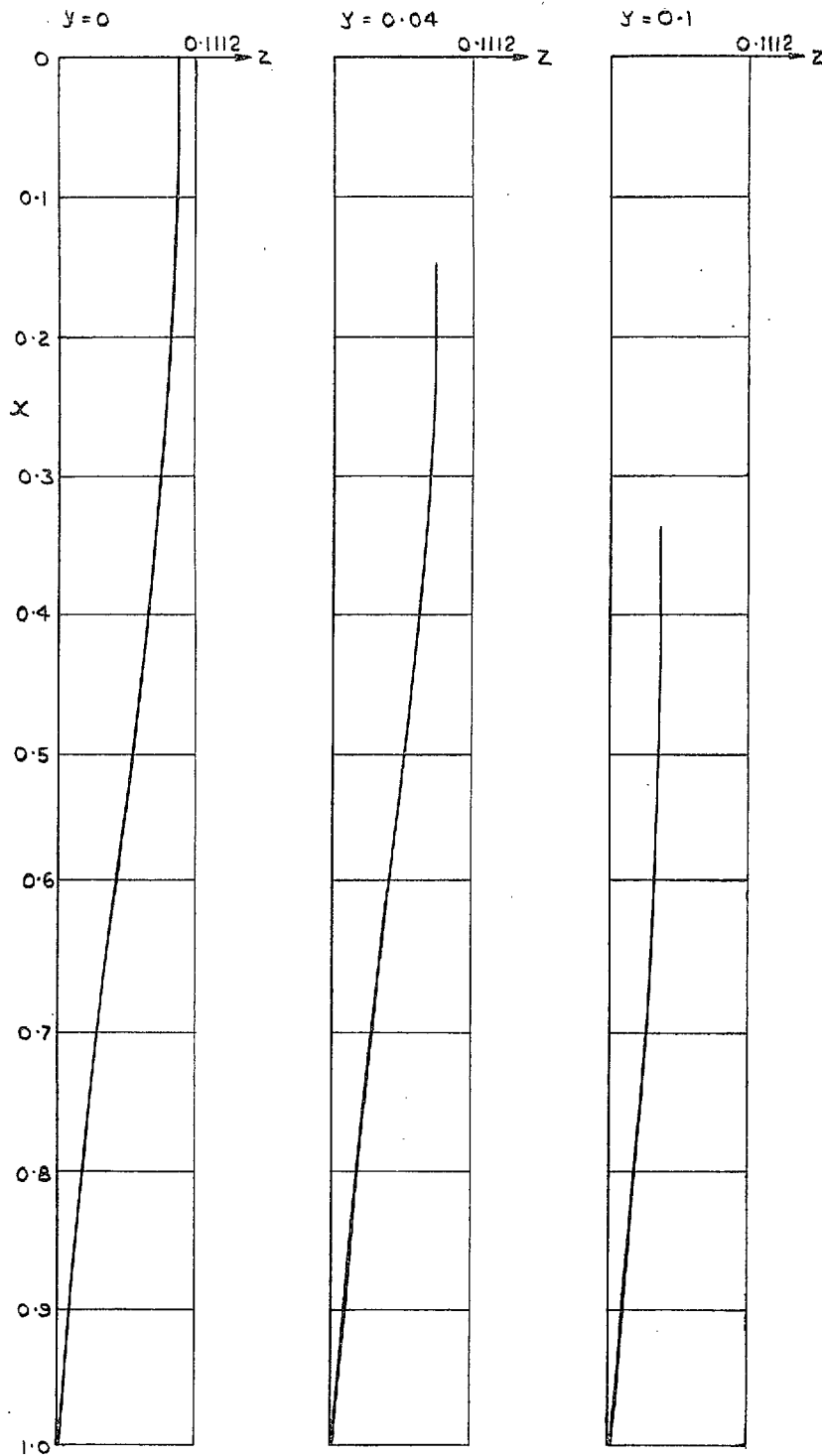


FIG. 4. Shape of camber surface of Wing 2.
 (Chordwise sections), $\gamma = 15$ deg., with no leading-edge pressure singularities at $M = 2.5$, $C_{L_0} = 0.1$.

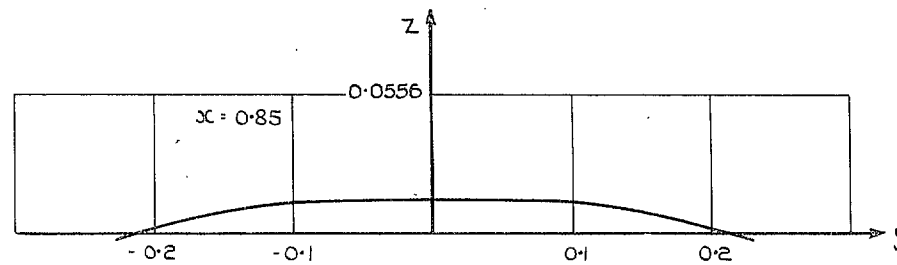
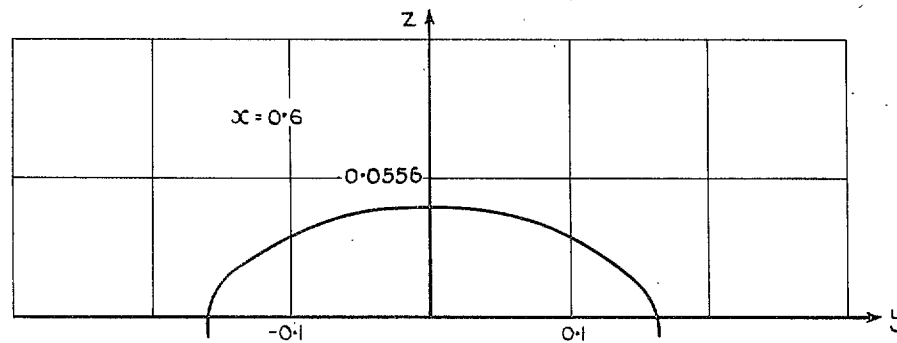
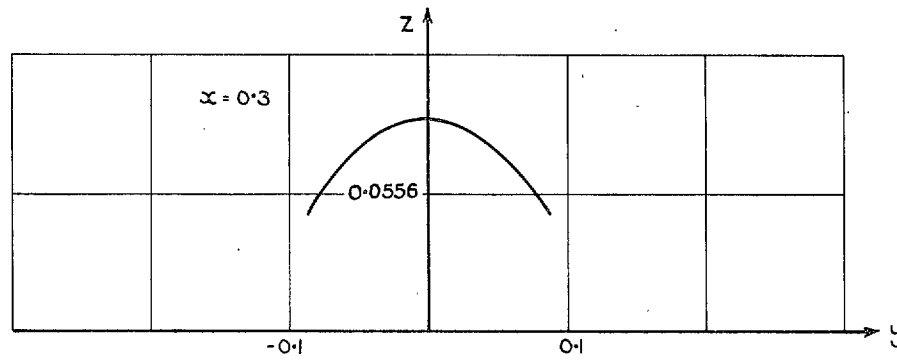
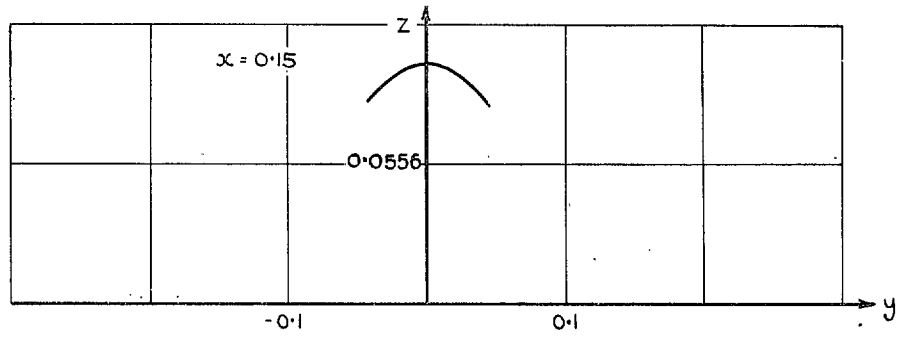


FIG. 5. Shape of camber surface of Wing 2.
 (Spanwise sections), $\gamma = 15$ deg., with no leading-edge pressure singularities at $M = 2.5$, $C_{L0} = 0.1$.

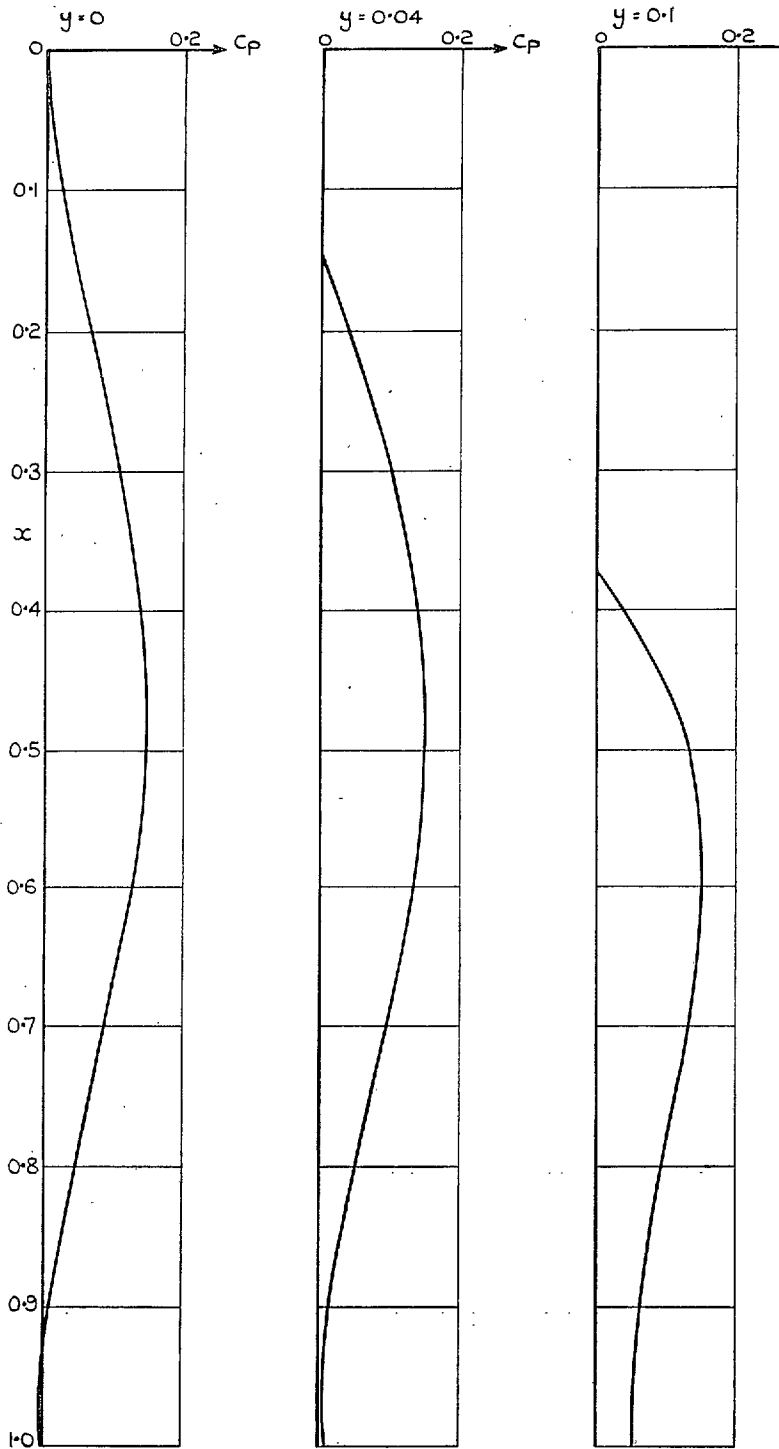


FIG. 6. Chordwise variation of loading coefficient of Wing 2, at $M = 2.5$, $C_{L_0} = 0.1$.

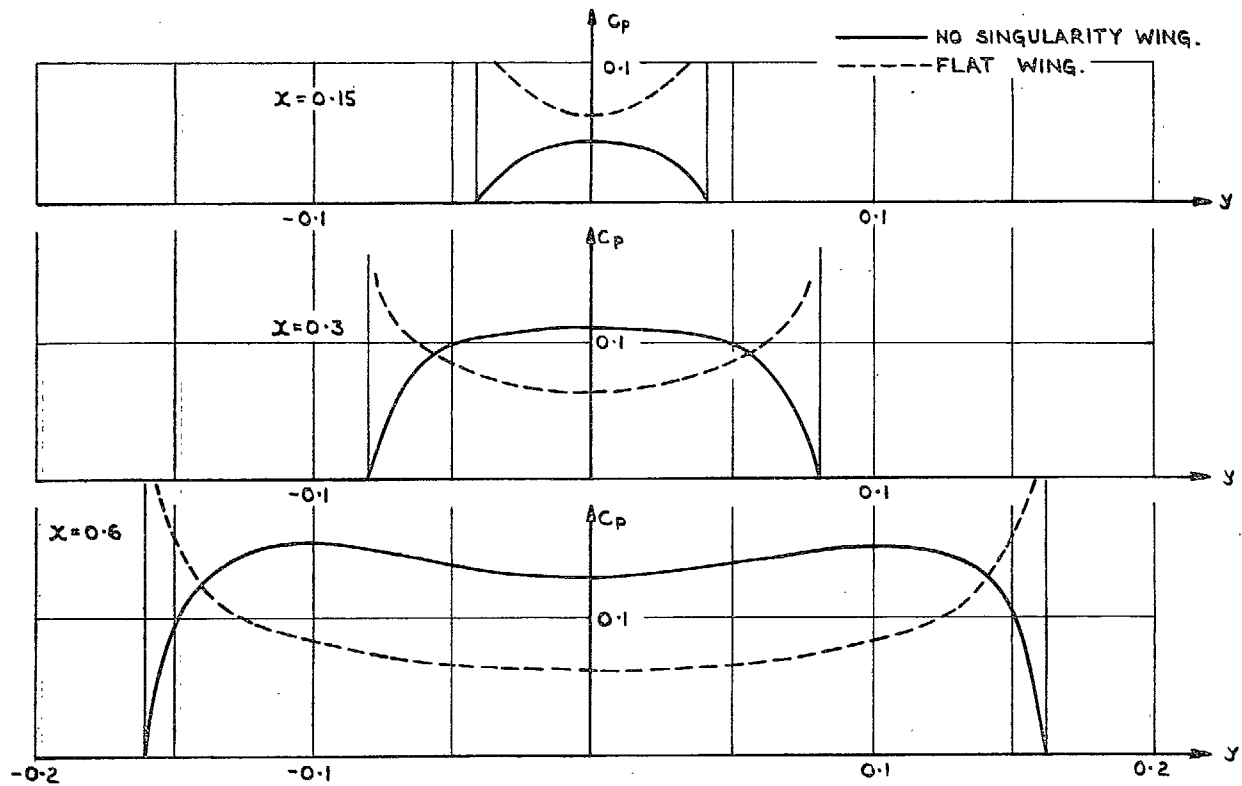


FIG. 7. Spanwise variation of loading coefficient, C_p , of Wing 2, at $M = 2.5$, $C_{L0} = 0.1$.

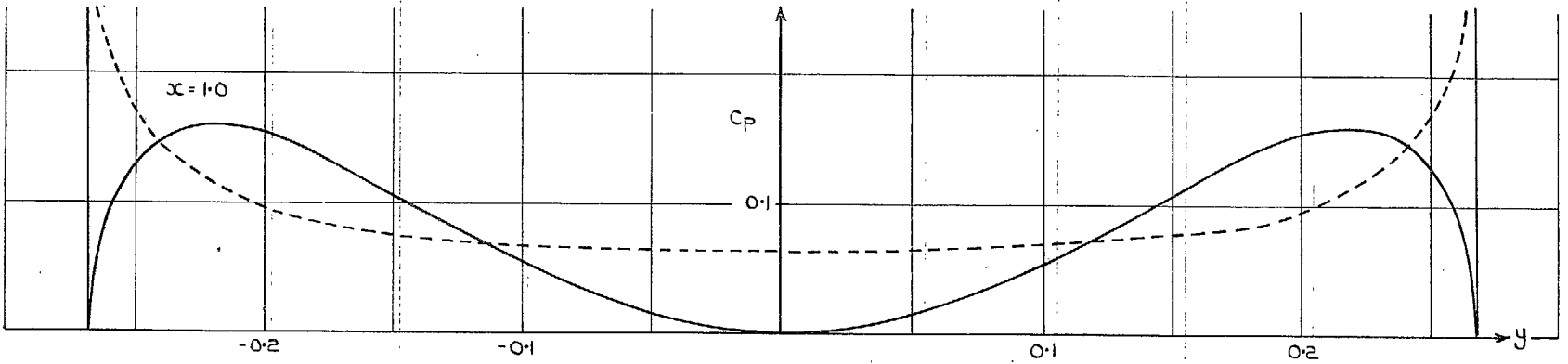
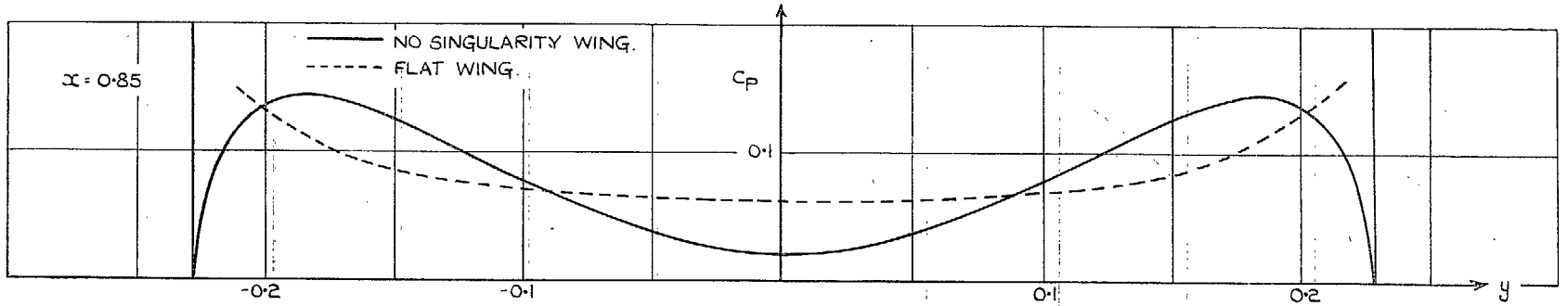


FIG. 7—continued. Spanwise variation of loading coefficient of Wing 2, at $M = 2.5$, $C_{L_0} = 0.1$.

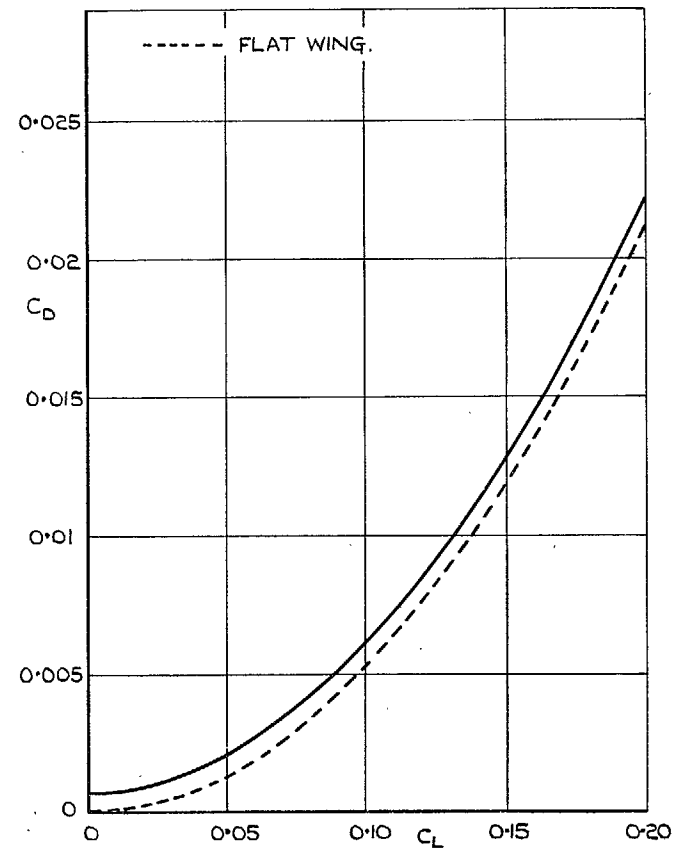
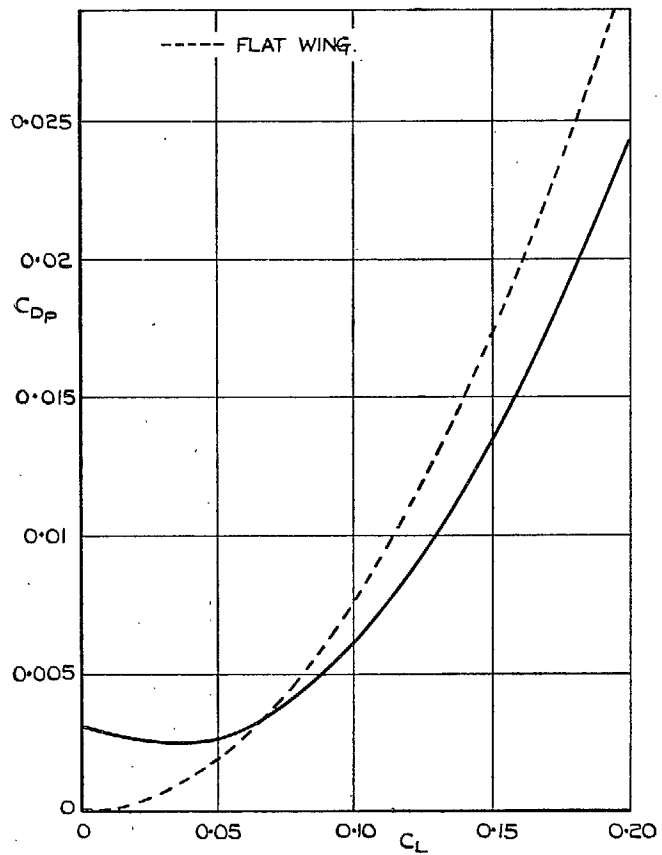


FIG. 8. Variation of drag with lift for Wing 2
($\gamma = 15$ deg.); design $C_L = 0.1$, $M = 2.5$.

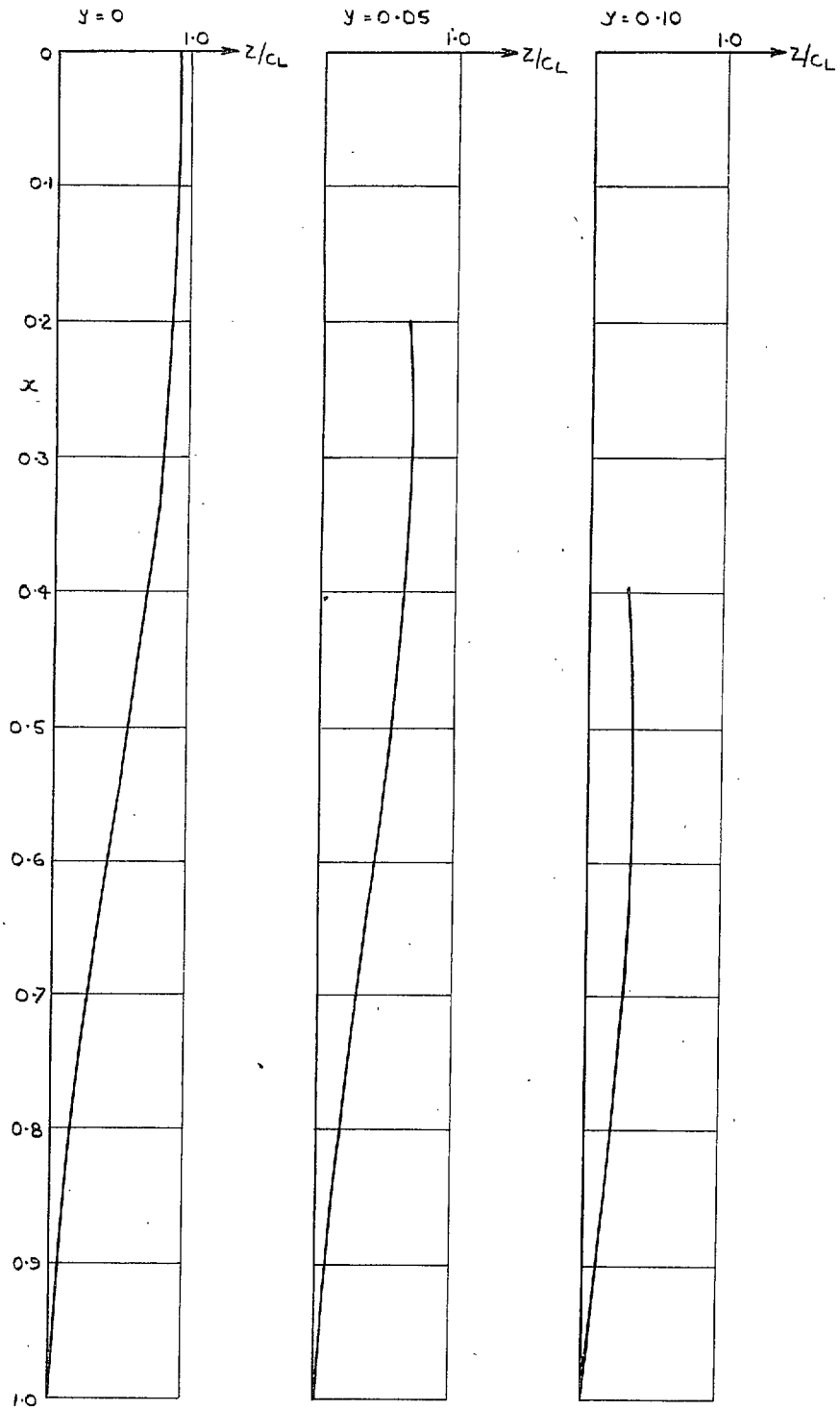


FIG. 9. Shape of camber surface of Wing 3.
 (Chordwise sections), $\gamma = 14^\circ 2'$ designed for minimum C_D/C_L^2 with no leading-edge pressure singularities at $M = 1.562$.

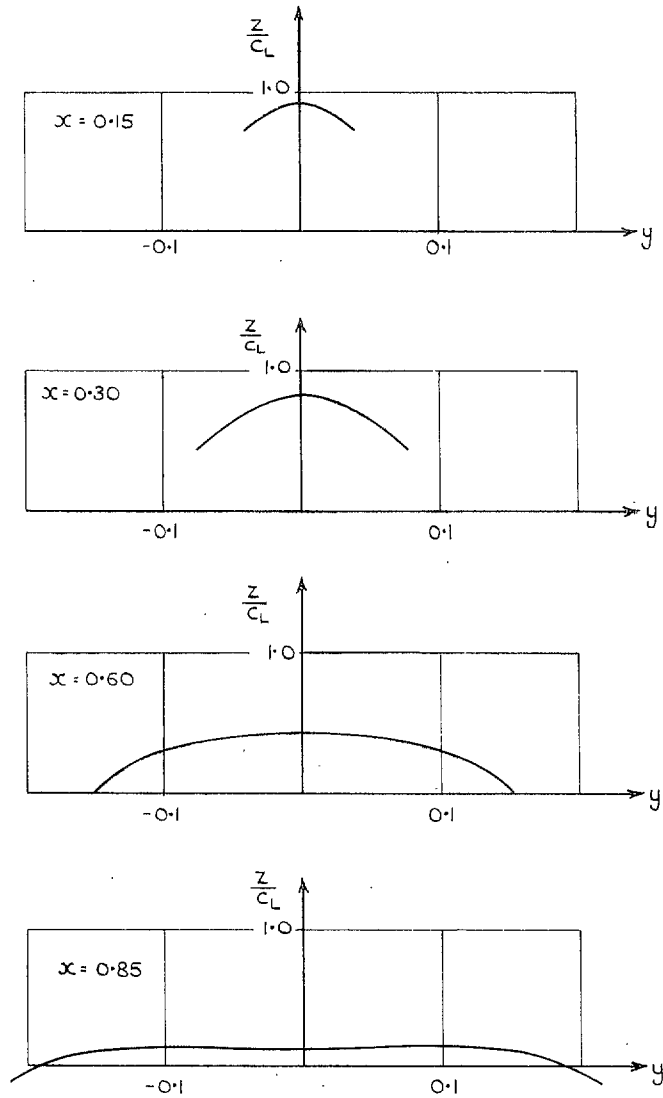


FIG. 10. Shape of camber surface of Wing 3.
(Spanwise sections), $\gamma = 14^\circ 2'$, with no leading-edge pressure singularities, at $M = 1.562$.

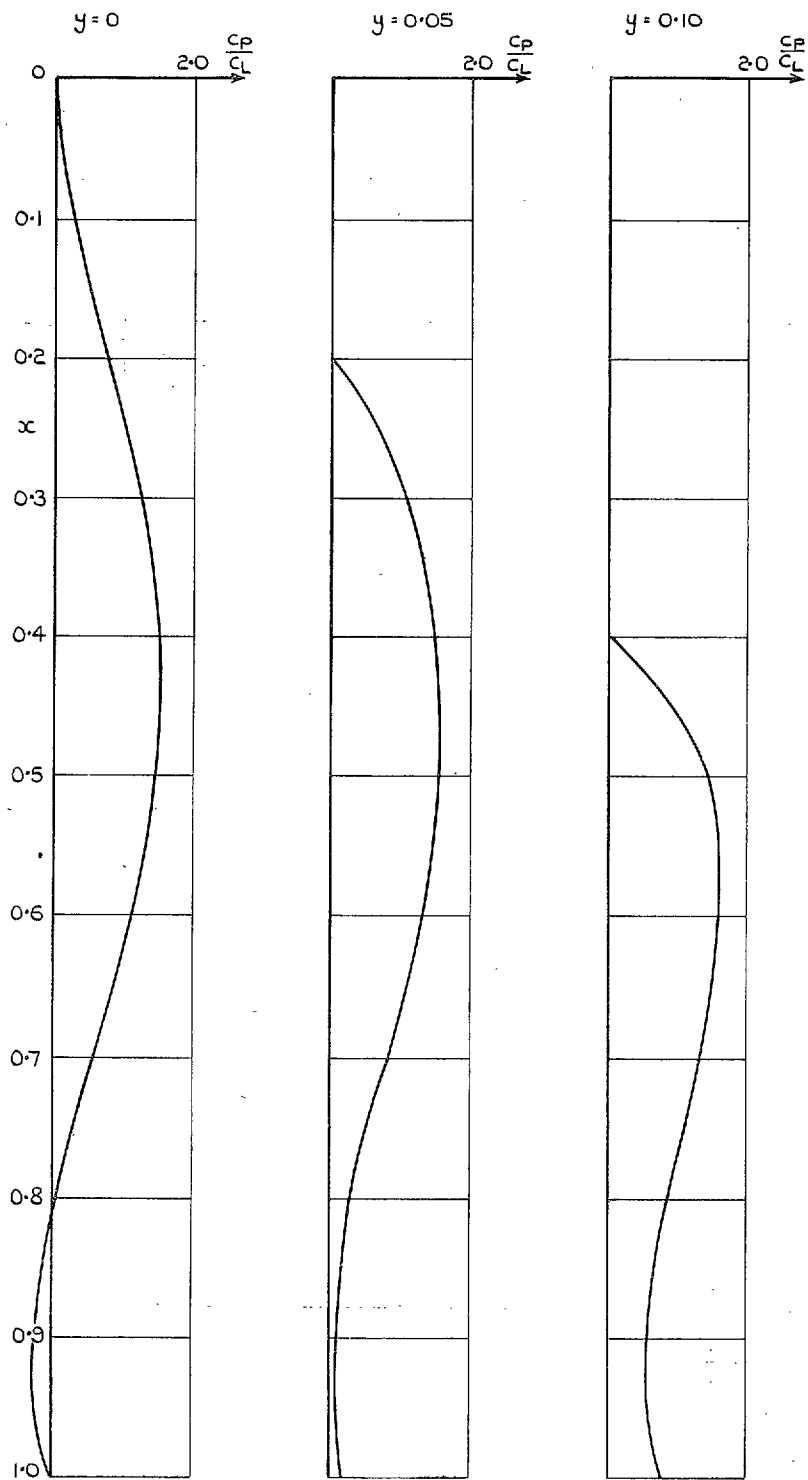


FIG. 11. Chordwise variation of loading coefficient of Wing 3, at $M = 1.562$.

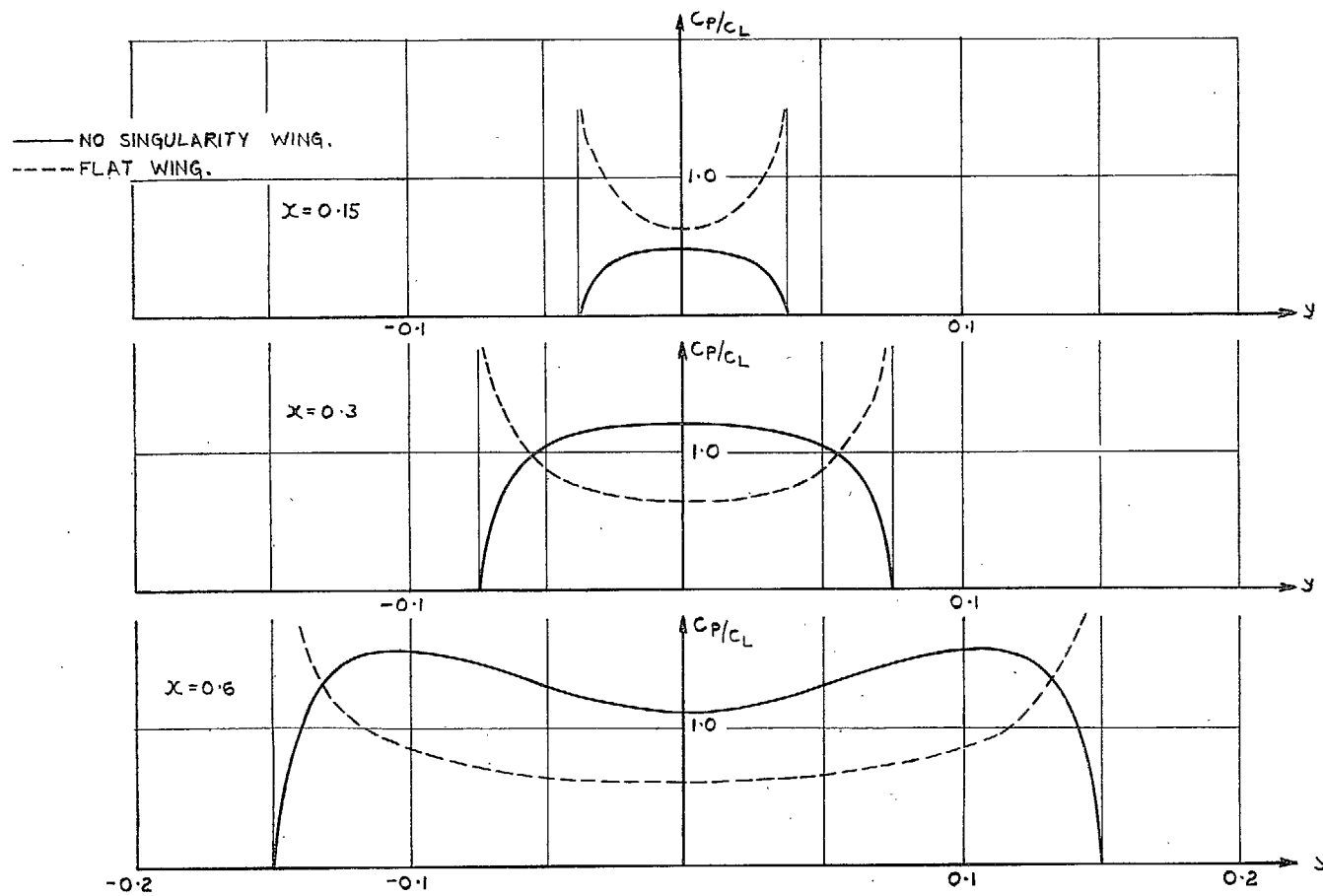


FIG. 12. Spanwise variation of loading coefficient of Wing 3, at $M = 1.562$.

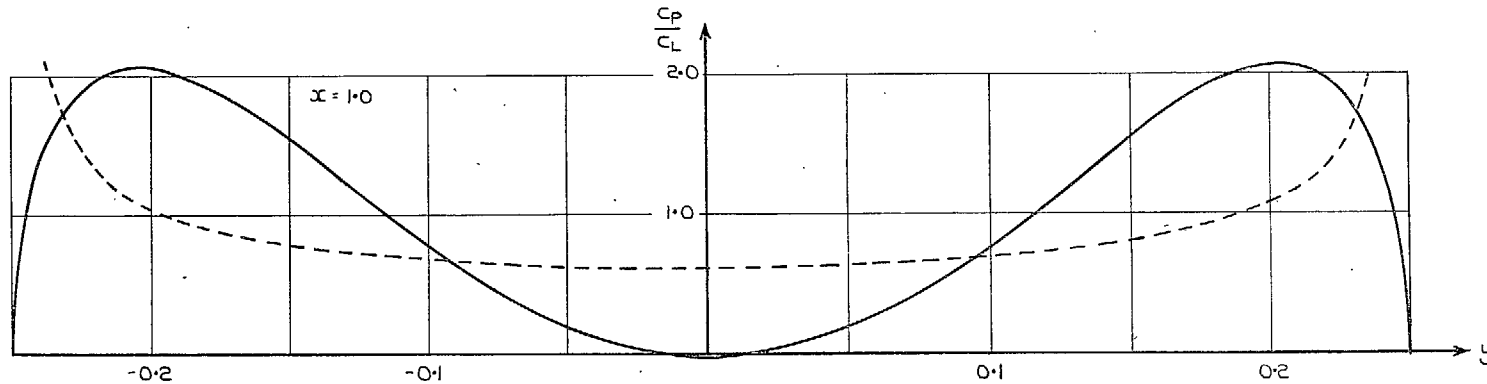
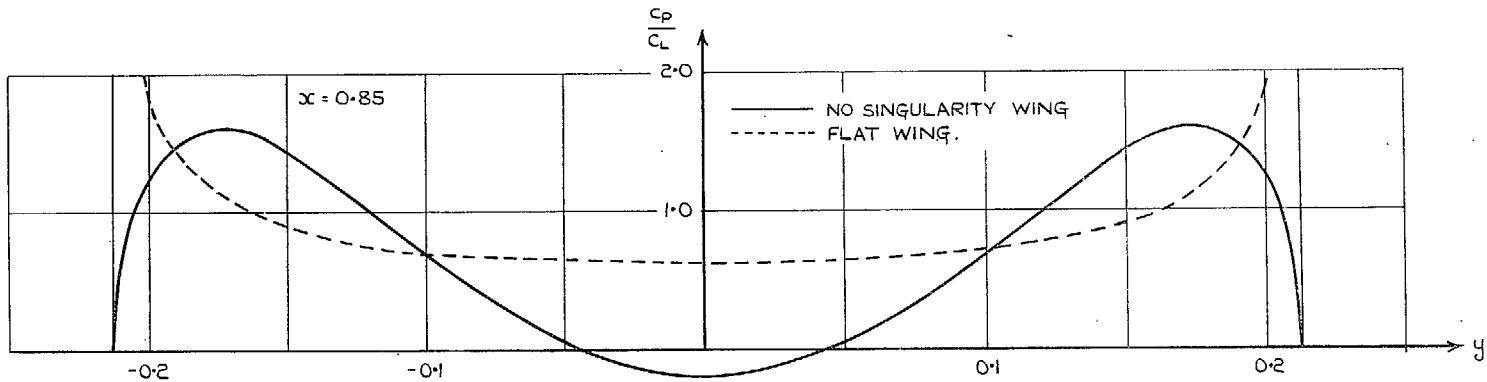


FIG. 12—continued. Spanwise variation of loading coefficient of Wing 3, at $M = 1.562$.

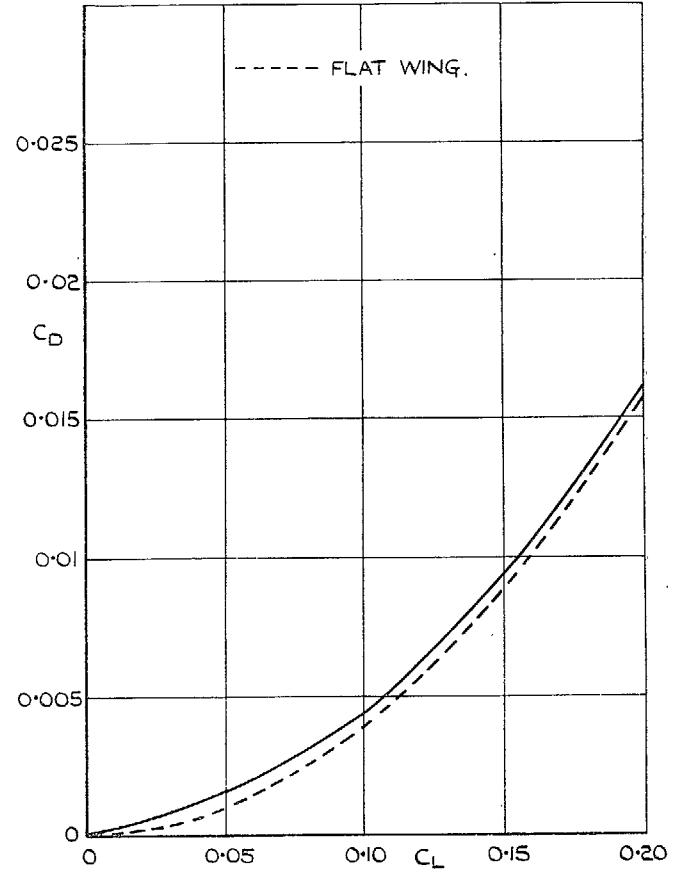
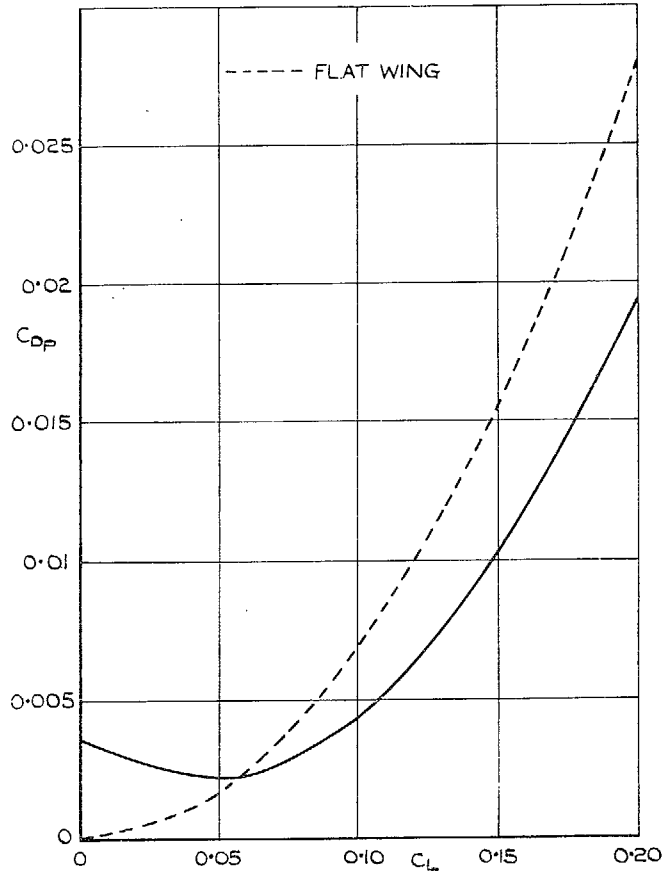


FIG. 13. Variation of drag with lift for Wing 3.
($\gamma = 14^\circ 2'$); design $C_L = 0.1$, $M = 1.562$.

© *Crown copyright* 1961

Published by
HER MAJESTY'S STATIONERY OFFICE

To be purchased from
York House, Kingsway, London w.c.2
423 Oxford Street, London w.1
13A Castle Street, Edinburgh 2
109 St. Mary Street, Cardiff
39 King Street, Manchester 2
50 Fairfax Street, Bristol 1
2 Edmund Street, Birmingham 3
80 Chichester Street, Belfast 1
or through any bookseller

Printed in England